CONTRIBUTION TO A TROPICAL CYCLONES TRACK FORECASTS

ARISING FROM A MODELS DYNAMICAL AND PHYSICAL COMPONENTS

Adam J. O'Shay
and T.N. Krishnamurti

Department of Meteorology
Florida State University
Tallahassee, FL 32306-4520

(Submitted on April 21th to Monthly Weather Review)

Corresponding Author's Address

Adam J. O'Shay
Department of Meteorology
Florida State University
Tallahassee, FL 32306-4520

Tel: 850 644 1746
Fax: 850 644 9642
e-mail: oshay@met.fsu.edu

ABSTRACT

The main goal of this study is to investigate the relative contributions from the components of dynamics and physics of a forecast model, toward the understanding of the recurvature dynamics of hurricanes. A number of experiments were conducted using the Florida State University Global Spectral Model (FSUGSM), run at a global resolution of 126 waves. A list of acronyms is presented in Table 2. The method of physical initialization was used to 'spin-up' the model, 24 hours prior to the five-day forecast period – thus better defining the initial water vapor, sensible heat fluxes and rainfall rates. A total of 4 cases were examined, two each for Hurricanes Cindy and Dennis - 12Z August 26 & 27, and 12Z August 28 & 29, respectively.

The usage of the FSUGSM employed a partitioning of the dynamics and physics into separate components, that assumes a residue-free budget of the models components. The model dynamics was broken down into a nonlinear advective component and also a linear dynamics (rest of the dynamics) partition. The model physics was partitioned into four components: deep convective heating, large-scale precipitation, total radiation and shallow convection & surface fluxes. The series of model runs were formulated to display the tropical cyclone forecast tracks, suppressing one or more of the partitions for each time-step, through day 5 of forecast. In one of our first models, the total dynamics (nonlinear advective + linear dynamics) was used to obtain the tracks of the cases – using the minimum sea level pressure as the storm center. The total dynamics component resulted in a weakly recurving track. The addition of the physics components incrementally sharpened the recurving track through time.

While the full model dynamics was used as a baseline, the results of this study indicated that the deep convection and total dynamics were an adequate combination to produce a recurving track for both hurricanes, for 50% of the four examined cases. The remaining cases required that the shallow convection partition be included along with the deep convection and the total dynamics. It was found that incremental improvements were seen with both the deep convection, shallow convection and the surface fluxes partitions, however the additions of the large scale precipitation and radiation in these partitions did not improve the track as compared with the full model, and their magnitudes were significantly smaller than the rest. The impetus for this study was based on previous partitioning work done on climate forecasts (Krishnamurti et al., 1996).

1. Introduction:

Significant contributions to the field of tropical cyclone motion have been made over the last half-century (Riehl and Burgner, 1950; Vanderman, 1962; Ooyama, 1964; Sanders and Burpee, 1968; Sanders *et al*., 1975; Hovermale and Livezy, 1977). Due in large part to advances in the computational sector of numerical weather prediction, the depth of understanding of a tropical cyclones internal dynamics and physics has increased dramatically (Kurihara et al., 1979; Madala, and Piacsek, 1975; Dong and Neumann, 1986; Krishnamurti et al., 1989; Krishnamurti et al., 1991b; Krishnamurti et al., 1998). Through the varying scales of tropical modeling, the theories of barotropic and baroclinic tropical cyclone development have been proposed and refined – these once undeveloped ideas have now become theoretical 'truths' within the tropical community.

The motivation of this study is to improve the understanding of a strong hurricane's internal dynamics and physics, as it undergoes a recurvature. Recurvature is simply the directional change that many tropical cyclones undergo where their motion goes from westward and poleward to eastward and poleward (for northern hemisphere tropical cyclones). A attempt to understand the contributions of particular dynamics and physics components is under-taken, while preserving a 'with and with' concept that allows the full non-linearity of the Florida State University Global Spectral Model (FSUGSM hereafter) to be explored (Krishnamurti, 1996). This study will employ a 'residue free budget' of sea-level pressure tendencies while integrating the model in a 'with and with' formulation that preserves the nonlinear interactions of the storm dynamics and physics.

Section 2 will provide an overview of the methodology of the FSUGSM and the partitioning strategy. Section 3 will review the data being used for the cases and section 4 will detail the results and analysis for four experiments.

2. Methodology

(a) The FSUGSM

The foundation of this study heavily involved the use of the FSUGSM – following Krishnamurti et al. (1998). The FSUGSM is a multi-level primitive equation global spectral model with spherical coordinates in the horizontal (?,f), where ? is the longitude and f is the latitude. The model employs a sigma (s) vertical coordinate where $s = \frac{p}{p_s}$,where p is the pressure and p_s is the surface pressure. All model runs in this study employed a T126 horizontal resolution (triangular spectral truncation), which is approximately 100 km in the tropics. An extensive outline of the FSUGSM is provided in Appendix 1.

(b) Model Code Formulation

Hurricanes Cindy and Dennis, both occurring during the 1999 Atlantic Hurricane season, were selected based on their observed recurving motion. We propose that the recurvature of these hurricanes can be broken down into a finite number of partitions, such that incremental contributions from each of the partitions will add to the final track of the recurving systems.

Our directive is a 'with and with' notion formulated within the model code. This concept is constructed from the principle that within a nonlinear model, the effects of the dynamical (advective and non-advective) and the physical forcings are fully inter-woven, that is – the dynamics and physics consistently co-evolve as functions of one another

throughout the model integration period. Based on this, the full model is run in parallel with 7 other versions the model that have a component suppressed during its integration. To maintain the 'with and with' notion, the model is integrated one time-step into the future, with the output of the full model stored and used as the starting point for the following time-step. Thus a 5-day integration yields 8 (full model run plus 7 partitions) unique configurations of the FSU-GSM for each time-step.

The above method is converse to the 'with and without' modeling procedure where the full model and full model minus a certain partition are run separately for several time periods - where the said difference at the end of the forecast period is due solely to the suppressed partition. This method is in error because we know that the model dynamics and physics continuously work with one another and co-evolve, so the model that is integrated forward in time, will seriously degrade the other fields through the selected forecast period – thus the 'with and with' concept achieves a far greater understanding of how the storm recurvature occurs via each particular partitioning component, while simultaneously maintaining the integrity of the fields. Figure 1. shows the track differences between using the 'with and with' technique employed in this study, against that of using a 'with and without' model integration scheme. The TDYN track is the full model dynamics track for the first experiment using the 'with and with' technique – tracking Cindy in a weakly recurving manner around the western side of the island of Bermuda. TDYN WWO is the full model dynamics using the 'with and without' technique. It can be seen that when the preservation of the nonlinear interaction of the dynamics fields are not maintained (TDYN WWO), there is severe degradation in the

skill of the track forecast – where there is no indication of a general barotropic (weakly recurving) storm motion.

In order to study the contributions from individual components of the FSUGSM, a series of experiments were made suppressing a specific portion of the model's dynamics or physics. The runs utilized the procedure described above and illustrated in Figure 2. This figure illustrates how the model is run with the seven other partitions each integrating for one time-step in the future, where the next time-step's started from the history of the parent run, or the full model. The design of the model runs was formulated from these model equations:

$$\frac{\partial \vec{V}}{\partial t} = -\left[\vec{V}\cdot(\nabla\vec{V}) + \dot{s}\frac{\partial \vec{V}}{\partial s}\right]_{AD} - \left[fk\times\vec{V} + RT\nabla q\right]_{RD} + \left[\vec{F}\right]_{PH} \tag{2.1}$$

$$\frac{\partial T}{\partial t} = -\left[\vec{V}\cdot\nabla T\right]_{AD} + \left[\dot{s}\frac{\partial T}{\partial s} + w\frac{RT}{C_p p}\right]_{RD} + \left[H_T\right]_{PH} \tag{2.2}$$

$$\frac{\partial S}{\partial t} = -\left[\vec{V}\cdot\nabla S\right]_{AD} + \left[\dot{s}\frac{\partial S}{\partial s} + \frac{w}{p}\left(\frac{RT}{C_p} - \frac{RT_d^{\,2}}{eL(T_d)}\right)\right]_{RD} + \left[(H_T - H_M)\right]_{PH} \tag{2.3}$$

$$\frac{\partial q}{\partial t} = -\left[\vec{V}\cdot\nabla q\right]_{AD} - \left[D + \frac{\partial \dot{s}}{\partial s}\right]_{AD} \tag{2.4}$$

Where $\vec{V}$ is the horizontal wind vector; T is the temperature; w is the p-coordinate vertical velocity; $\dot{s}$ is the s vertical velocity; q = ln p_s, p_s being the surface pressure; S =T – T_d, dewpoint depression; $\vec{F}$ are the frictional effects; H_T is the diabatic heating effect; H_M is the moisture sources and sinks effect; R is the dry air gas constant; C_p is the specific heat of air at constant pressure; and $L(T_d)$ is the latent heat of water/ice at

temperature T_d (Krishnamurti et al., 1996). Equations 2.1 – 2.4 represent the model momentum equation, the thermodynamic equation, the moisture equation and the continuity equation – all in the sigma coordinate, respectively. The momentum equation (2.1) is then transformed into two separate equations, the Vorticity equation (obtained by operating $\vec{k}\cdot\nabla\times(2.1)$), and the Divergence equation (operate $\nabla\cdot(2.1)$). This produces five equations total schematically shown by:

$$\frac{\partial V}{\partial t} = F_V(AD) + F_V(RD) + F_V(PH) = F_V \tag{2.5}$$

$$\frac{\partial D}{\partial t} = F_D(AD) + F_D(RD) + F_D(PH) = F_D \tag{2.6}$$

$$\frac{\partial T}{\partial t} = F_T(AD) + F_T(RD) + F_T(PH) = F_T \tag{2.7}$$

$$\frac{\partial S}{\partial t} = F_S(AD) + F_S(RD) + F_S(PH) = F_S \tag{2.8}$$

$$\frac{\partial q}{\partial t} = F_q(AD) + F_q(RD) + F_q(PH) = F_q \tag{2.9}$$

where F(AD), F(RD), and F(PH) are the forcings due to the non-linear advective dynamics, the rest of the dynamics, and the physical processes, respectively, with F being the total forcing for each particular equation. In the above equations (2.5-2.9) the terms within the brackets marked by AD, RD and PH represent the partitions of nonlinear advective dynamics, the rest of the dynamics, and the total physics, respectively. The total physics is then broken up into the aforementioned partitions, described above.

(c) The Partitions

While maintaining the notion of the 'with and with' concept, the model code is set to integrate one time-step into the future, with output from the full model and the partitions retained for tendency calculation. Simply put, the model code creates a one time-step forecast of the full model, the full model minus non-linear dynamics, full model minus deep convection and so on through the list of partitions. At the end of each time-step, the full model output is used for the starting point of the next time-step forecast. At the end of the 960 time-step (120 hours) integration, the tendencies between the full model forecasts (FM) and the full minus a partition (FMP) are accumulated for all the time-steps and all the partitions. Specifically:

$$\text{Partition P Tendency} = \sum_{1}^{t} (FM - FMP)_t \qquad (2.10)$$

This accumulation of a particular partitions' tendencies over the course of a specified time, t, will provide the contribution of that partition to the total field, through time t. The accumulation can be done over any specified time – for our purposes we will typically be looking at the 24-hour tendencies throughout the course of the 5-day forecast.

An important consequence of the 'with and with' technique is that the summed total of the physics tendencies and the dynamics tendencies will equal the total, full model tendency – assuring that the model is creating a residue free budget of the dynamics and physics.

(d) Model Physics Consistency

This section examines the model's physics components. As mentioned previously, the partitions were formulated such that, their exists a full physics run where no

components of dynamics were included, in addition to the four components of the physics, run as separate cases. We shall first show some contributions to the total physics components of the model (pressure tendencies) and for of each of the individual components of the model (deep convection, radiation, shallow convection, large-scale precipitation). Table 1. shows the values of the total physics run and the summed total values of the each of the physics partitions – the units of the table are in hPa per 120 hours (these values are for the 120-hour forecast cases for both Cindy and Dennis). The values for each of the total physics cases are within 0.20 hPa to their summed physics counter-parts – indicating the model is very nearly conserving the total pressure tendency from the partition computation. These are values based on the 'with and with' concept.

3. Data

This study employed 0.5° degree ECMWF gridded data, available once daily, at 12Z, through the storm periods of Hurricane Dennis (August 26-29, 1999) and Hurricane Cindy (August 27-28, 1999). The ECMWF data was interpolated to a spectral resolution of T126, where the global grid size is 0.9375° (384 x 192).

The model topography was obtained using a high-resolution (10' x 10' latitude-longitude mesh) terrain field compiled by the U.S. Navy. The mean of the high-resolution terrain within a 1° grid square is computed to represent the topographic surface heights. This field is then interpolated to the Gaussian grid, at T126 resolution. A consistency check is performed comparing the land-sea mask and the model topography to assure that the grid points over water have a zero height and land grid points have a minimum height of 10 meters. The orographic field is spectrally truncated, similar to other model variables, at the T126 horizontal resolution.

The SST data used is the optimal interpolation (OI) for the sea surface temperature analysis produced by the National Centers for Environmental Prediction (NCEP) (Reynolds and Smith 1994). This analysis is on a 1° grid and uses in-situ and satellite SSTs plus SSTs simulated by sea-ice cover. These SST data-sets were interpolated to the Gaussian grid points at the T126 horizontal resolution.

The albedo field, also provided by ECMWF, was a base climatology defined for the northern hemispheric summer – this too was an interpolated field to the T126 resolution. Further information as well as displays of the SST, albedo and the terrain fields can be found in Krishnamurti et al. (1995).

4. Results and Analysis

(a.1) Partition Tendencies of Cindy – Case #1

Figure 3. shows the full model, FSUGSM forecasts and the best-track (observed) positions for Hurricane Cindy, obtained from the NHC/TPC. Cindy recurved near 58.5° longitude, where the storm moved northwest for the first 48 hours, then followed by a 24-hour period of nearly pure northward motion. This northward motion ended as Cindy began to accelerate toward the northeast, where the NHC/TPC deemed it extra-tropical and said to be merging with a stronger low-pressure area by the 120-hour time-period. As a result of this extra-tropical transition, there are no observation points beyond 12Z, 31 August 1999, the 120-hour marked position. This experiment was integrated out to five-days where the recurvature of Hurricane Cindy occurred approximately at the mid-way point.

Sea-level pressure tendency computations were performed for 24 hourly time periods, through the length of the model integration. Figure 4. depicts the full model sea

level pressure tendency for 24, 48, 72, 96, and 120 hours and is listed as a benchmark for examination of the rest of the partitions. Each of the five figures builds from the one previous, i.e. the pressure falls and rises depicted in 4.b result from a summed difference of the full model and the starting point from the first 24 hours (figure 4.a) up through 48 hours, and so on for each figure through 120 hours. Thus these are time accumulated pressure tendencies. Figures 5 – 11 illustrate the various partitioned components of the full model. These figures depict the pressure tendencies if only those specific components were run in isolation from the remainder of the model components.

Visible in figures 5 and 6 are values of the pressure tendency that are significantly larger than that of the full model pressure tendencies for each time period. Magnitudes for the pressure tendencies in the vicinity of Cindy range from –400 hPa to over 500 hPa per time period – indicating that if the model is left to run with only one of these components, pressures will vary widely to both the positive and negative. The non-linear advective dynamics illustrates an interesting coupling when compared with the linear dynamics. Looking only at the 24 hour time period of both figures (5a and 6a) it becomes clear that where the nonlinear dynamics may show a negative pressure tendency (falling pressures through time) the linear dynamics acts to counter this fall with a positive pressure tendency. This pattern was found for all cases and occurs as a consequence of the modeled balance of the vorticity and divergence equation. The figures in general show a tendency for pressure falls (rises) by one component to be at least marginally countered by pressure rises (falls) from the other component of the dynamics. A closer examination of figures 5 and 6 reveals that the largest magnitude gradients of the isallobars were found over land areas – particularly over the rugged terrain of Hispaniola

and the extreme northern portion of the Appalachian Mountains, in the upper left region of the figures. Although the pressure tendencies are smoother in the vicinity of Hurricane Cindy, reasonably tighter packing of the isallobars did exist in the later forecast periods.

Figures 7-11 comprise the pressure tendencies for the physics components of the model integration. The total physics sea level pressure tendency is shown in figure 7, where the model was run with only complete model physics, where both components of dynamics were suppressed. Distinctly visible for all time periods are the pronounced negative pressure tendencies as Cindy progressed through its recurving track. Within the first 24 hour time period (7.a), pressure falls near 26N / 55W were on the order of 60 to 100 hPa – centered in a very localized region – indicating that the total physics is contributing to a large decrease in the central pressure of Cindy. This result is not surprising since many studies have found that the warming of the tropospheric column in the region of a hurricane eye-wall, largely due to physical processes, is the fundamental cause of a Tropical Cyclone's (TC) low central pressure (Shaw 1922; Palmen 1948; Holliday and Thompson 1979; Anthes 1982). The remaining time periods of figure 7 are consistent with the northwestward extension of the negative pressure tendency, followed in the later periods by a north-northeast decrease of the total pressure. Note that in the later time periods, the region of pressure falls that occurred in the early time periods may still remain visible, however there may be an elongated negative pressure tendency that illustrates where and how deep the storm became over the specified time period.

Very strong similarities are seen between figure 8. (deep convection tendencies) and the total physics figure, 7. The total physics sea level pressure tendencies are analogous in both placement of the negative pressure tendencies and in magnitude – as

seen in each time period through the five day forecast. For this five day forecast, in general, the deep convection pressure tendency contributes the most to the entire total physics accumulated pressure tendency change. This statement is supported further through examination of figures 9-11 (large-scale precipitation, radiation and shallow convection), where the magnitudes of these sea level pressure tendencies are at most on the order of ± 16 hPa (with these higher values arising from the shallow convection partition) – significantly less than the deep convection partition pressure tendencies. The tendencies arising from radiation and large-scale precipitation are the smallest of the partitions examined here, with magnitudes only near ± 3 hPa. The large difference among the partition tendencies between deep convection and the others can be attributed to the nature of the atmospheric phenomena that we are studying (i.e. a convectively vigorous hurricane). The remaining physics partitions, aside from deep convection, do play some role in the overall total physical component, however the magnitude as seen here is significantly smaller, and sometimes less than two magnitudes in value.

(a.2) Partition Tracks

This section will examine the tracks of the aforementioned partitions. All of the tracks will include at least the total dynamics – both the nonlinear advective dynamics and the rest of the dynamics are portrayed within. The directive here is to examine how the addition of the partitions, in various combinations, will change the tracks of the sea level pressure minima (used as the storm center) through the course of the five-day forecast.

Various combinations of partitions, and the full dynamics track provides a total of 17 tracks plus the full model track. An initial examination revealed that the previously

suggested strong dominance of the deep convection could help to separate out the tracks from one another. Figure 12. shows the full model plotted track in addition to all the partitions with the full model dynamics and deep convection. It should be noted that the difference between DLRS and PHY is subtle. The DLRS track originates from adding the pressure tendencies from each component of the physics, since they were each separately created during the model runs; the PHY track was created during the full physics run, where both components of the dynamics were suppressed. A closer examination of figure 12. reveals that the full model run is most closely followed by the total physics run, that includes the full dynamics. It can also be seen that the track due to just deep convection had the furthest west recurving track of all, while the full model was furthest east – thus incremental track improvements were seen through the addition of certain combinations of partitions. Aside from the full model forecasts (DLRS and PHY), the three closest recurving combinations of partitions were: DLS, DS, DRS. In contrast, combinations DR and DL both had recurving tracks further west of the three aforementioned tracks. It appears that the common denominator among the 'next-closest' combinations is the shallow convection partition. The strong contribution from the shallow convection is seen along with deep convection (DS), having approximately the same track as DLS – suggesting that the non-convective precipitation physics is doing little to change or improve the track of Cindy through the recurvature phase.

Figure 12. also illustrates the nearly identical tracks of the partitions through the track position near 30N / 64W (near 72 hours – 12Z, 29 August). The deep convection track continues generally northwest, while the DR track bends just east of DC. Track

DLR and DL both nearly mimic one another, recurving Cindy just west of the island of Bermuda.

The four tracks without shallow convection also experience an eastward and southeastward motion in the last 36 hours of the 120-hour forecast. This southeast motion suggests a loss of continuity with respect to the full model forecast track – where all tracks with shallow convection do not have this south and east component of motion. The shallow convection partition has been seen as a significant contributor to the total track forecast – where it alone with deep convection created a forecast track nearly identical to those with radiation or large-scale precipitation as well.

Figure 13. contrasts to the previous figure in that it includes only those tracks that do not have deep convection as one of their components. Comparing the tracks seen in figure 13. and those of figure 12, it is clear that the addition of deep convection to the track is a vital component for storm recurvature. In all of the cases in figure 13, not one of them exhibits any strong form of recurvature – though during the last 24 hours there is a slight indication of storm motion toward the northeast. The motion of these tracks in figure 13, moving in a weakly recurving motion through day 5 of forecast indicates that the subtropical ridge is a dominant steering mechanism here (primarily in response to the model equations relating to the vertically integrated, deep layer wind-field driving the storm motion) however the lack of an incremental improvement in the track from all three (L, R, S) partitions was quite surprising. Figure 13 illustrates that the combined effects of the large scale precipitation, the radiation and the shallow convection do not provide a more skillful storm motion forecast, compared with only the total dynamics forecast. This result does not suggest that these three components are unimportant in the

full model prediction system – on the contrary, it is non-trivial to be mindful that the coupling of these various partitions can lead to very skillful forecasts, as we saw in figure 12, where the deep convection and shallow convection coupled together to produce a very skillful forecast, relative to the full model forecast.

(b) Experiments 2-4

For the remaining three cases we will examine only the partition tracks for each experiment – illustrating the incremental improvement of the recurving track of the storm from the addition of the model components.

The second experiment for Hurricane Cindy was initiated 48 hours prior to the observed and forecasted recurvature. At this point the motion remains mostly northwest, with a weakening in the mid-Atlantic ridge, that appeared to influence Cindy's increasingly northward motion. The full model and individual partition components sea-level pressure tendencies (not shown) illustrate strong similarities to those of the previous experiment. By day four of forecast, the storm was aggressively transitioning to an extra-tropical cyclone as it raced northeast toward the northern Atlantic Ocean. Figures 14 and 15 illustrate the partition tracks for this final case for Cindy. These tracks exhibit spatial and temporal similarities to those of the previous case. The full model begins near 27N and 55W and begins to move north along near 31N and 60W. While several of the partition tracks in figure 14 do exhibit a recurving track similar to the full model, a large cluster of tracks move toward 34N/62W and remain in place through the rest of the forecast period. A closer examination of the recurving tracks reveals that each one contains the shallow convection partition. This is very similar to the previous case with Cindy, where the tracks became much improved with respect to the full model forecast,

when shallow convection was an included as a member of the combinations. What differs with this case as compared to the previous is that the DC track does not recurve here. That is, deep convection alone does not produce a recurving track – it requires the input from the shallow convection partition to complete the recurvature.

Figure 15 shows tracks that are comprised of the combinations of partitions that did not include deep convection. The tracks shown in this figure all have a similar five-day forecast tracks towards northwest motion for the first three to four days followed by motion toward the north for the remainder of the time period. This figure again suggests that the addition of partitions to the full model dynamics, alters the full dynamics track very little if deep convection is not part of the set of the included partitions.

The two cases for Hurricane Dennis saw similar patterns of pressure partitioning as for the Cindy experiment, within the isallobaric fields. The partition tracks for this first case were again divided into those that included deep convection and those that did not. Figure 16, illustrating tracks with deep convection, show that all of the tracks recurved Dennis, without bringing the storm ashore during its northeast motion. The outer recurving track, DC, recurved Dennis near 30N/80W and had the highest track error during the recurving time periods. It can be seen that the DR track provides a slightly improved track as compared with DC. Better still, are the DL, DLR, DS and DLS tracks. Aside from the full model (DLRS or PHY), the closest partition-forecasted track to the full model was the track from DLS. Regional budget computations revealed that large-scale precipitation partition is exhibiting a dramatic influence over the track positions, as compared with the cases for Hurricane Cindy.

The illustration of those tracks that do not include the effects of deep convection, in figure 17, show little resemblance to the full model forecast –they move Dennis mostly due west for the first 6-18 forecast hours, and remain over the peninsula of Florida. This figure indicates the dominance of deep convection among the partitions, as recurvature occurs in the observed data set and is confirmed by our full model forecast.

The partition tracks for the final case of Hurricane Dennis are shown in figures 18 and 19. Figure 18 illustrates a set of tracks that move in two directions. One set follows the full model during its recurvature, and another set moves Dennis towards the extreme southeast North Carolina while bending the storm toward the northwest there after. The four tracks that bring Dennis into North Carolina are DL, DC, DR, and DLR – all tracks that do not contain the shallow convection partition. The remaining tracks comprise the remaining partitions all containing the deep convection and shallow convection & surface fluxes partition. It appears that this model forecast is consistent with one of our experiments with Cindy where we had noted that having deep convection as a member in the partitions was not necessarily sufficient to yield a storms recurvature. The contribution from the shallow convection was considerable and necessary for the storm to turn back toward the northeast. Within the first 12 hours of this case, figure 19, the entire set of tracks moved south-westward toward the northeast Florida coast and Dennis was located to the north and northeast over land. The spread among the tracks in figure 19 is fairly minimal since they were fairly poor representations of the full model forecasts.

(c) Partition Track Errors

Employing a great circle approximation following the Haversine formula (Sinnott, 1984), track errors were computed for each of the four cases examined here - where the

full model was used as a reference forecast. The average of the two cases for each of the storms was computed with the partitions broken into the same two groups used to illustrate the partitioned tracks, illustrated in the previous sections. Figures 20, 21, 22 and 23 show the Hurricane Cindy and Dennis two-case averaged track errors for the deep convection & dynamics components and the other physics partitions (besides deep convection) & dynamics components, respectively.

When comparing the track errors between the two storms several interesting features become apparent. In figure 22 we note that the track errors for the partitions without shallow convection are higher (by 200 to 400 km) than for those in figure 20, for time periods through 84 hours. The track errors for the partitions with shallow convection exhibit similar values through 84 hours, however in the longer term, the errors for Hurricane Dennis were larger than those of Cindy. Larger track errors in the early to middle time periods were seen for Hurricane Dennis, for the partitions that did not include deep convection – here the values were greater by more than 350 km in some cases.

5. Conclusions

The main goal of this study was to investigate the relative contributions for the components of dynamics and physics of a forecast model, and for the understanding of the recurvature dynamics of hurricanes. The 'with and with' partitioning technique employed here is an extremely useful procedure for model output diagnosis in numerical weather predicition modeling. This procedure enables us to examine the physical and dynamical processes that occur while exhibiting nonlinear couplings among the different model components. The experiments performed here preserve this nonlinear notion and

all effects of component estimations maintain the model consistency and atmospheric non-linearity while casting residue free budgets of the hurricane pressure tendency.

The computation of the tendency charts and the budgets (not shown) for each of the time periods were carried out to provide a spatial and quantitative feeling for how the partitions of the physics and dynamics of a model each contributed to the overall full model sea level pressure tendency. The partition tracks are the new findings of this study. Examination of all of the partition tracks for both Cindy and Dennis provide several insightful conclusions on the individual components of the model, studied here. Initial tests of the partitioned tracks reveal that a division of them into two separate groups would prove useful: those that contain the total dynamics and deep convection along with varying combinations of other partitions, as well as the total dynamics coupled with combinations of partitions excluding deep convection. The full dynamics based partition tracks provided a atmospheric steering baseline for the storm diagnostics presented here.

For both of the cases for Hurricane Cindy, significant track improvement were noted from the addition of shallow convection to the partitioned contributions and combinations. For the first case, the track improved by nearly 150 km near the point of recurvature, where track DS recurved Cindy east of Bermuda, where DC track kept it west of the island. It can be said that the entire difference in these two tracks is from the contribution of shallow convection – since our method is able to extract such information.

The two experiments performed with Hurricane Dennis exhibited rather similar results as those from Cindy. Improvements with the addition of shallow convection to the partition combinations were seen, particularly in the second case, where the tracks without this partition moved the storm mostly north and toward inland areas in extreme

southeast North Carolina. Here again, all the tracks that included deep and shallow convection recurved, with varying degrees of skill as compared to the full model forecast. The significant contribution from the shallow convection and surface fluxes partition can also be attributed to the movement of this storm over the warm Gulf Stream that was also oriented along the actual full model's track. This potential air-sea interaction was, most likely, a significant contributor to the shallow convection and surface fluxes partitions – resulting in a very large increase in the magnitudes from this component in the partitioning for this storm.

The experiments performed within this study have been generalized as much as possible, in that the conclusions were aimed to provide, for the first time, an indication how the diagnosis of a fully non-linear model partitions the history of a recurving hurricane. We found that the deep convection portion of the total physics dominates the sea level pressure tendencies, with shallow convection, non-convective precipitation physics and radiation having their respective rank-ordered contributions. In general, the total dynamics contributed considerable variability for the sea level pressure tendencies, the total dynamics alone did not produce a significantly recurving track for these two storms. It was with the addition of deep convection among the partitions, we started seeing the successful forecasts of the sharpened recurving storm motion. Thus the total dynamics and deep convection appear to be necessary components for recurvature for these hurricanes, however in two of the cases these alone were not sufficient. The addition of the shallow convection & surface fluxes partition contributed to the completion of these recurving tracks.

6. Acknowledgements

The research conducted here has been supported NSF grant ATM-010874. The authors wish to express sincere appreciation to the European Center for Medium Range Weather Forecasts (ECMWF) for providing analysis data-sets employed in this study and also to the late Dr. H.S. Bedi for significant contributions made to this research.

References

Aberson, S.D., and M. DeMaria, 1994: Verification of a Nested Barotropic Hurricane Track Forecast Model (VICBAR). *Mon. Wea. Rev.*, **122**, 2804-2815.

Anthes, R. A., 1982: Tropical cyclones, their evolution, structure and effects. *Meteor. Monographs*, **19**(41), 208.

Arakawa, A., and W.H. Schuber, 1974: Interaction of a cumulus cloud ensemble with the large-scale environment. Part I. *J. Atmos. Sci*., **31**, 674-701.

Baer, F. 1964: Integration of the spectral Vorticity equation. *J. Atmos. Sci*., **21**, 260-276.

Bennett, A.F., L.M. Leslie, C.R. Hagelberg, and P.E. Powers, 1993: Tropical cyclone prediction using a barotropic model initialized by a generalized inverse method. *Mon. Wea. Rev*., **121**, 1714-1729.

Businger, J.A., J.C. Wyngaard, Y. Izumi, and E.F. Bradley, 1971: Flux profile relationship in the atmospheric surface layer. *J. Atmos. Sci*., **28**, 181-189.

Cavies, R., 1982: Documentation of the solar radiation parameterization in the GLAS climate model. NASA Technical Memorandum 83961, Goddard Space Flight Center, Greenbelt, MD.

Chang, L. W., 1978: Determination of surface flux of sensible heat, latent heat, and momentum utilizing the bulk Richardson number. *Papers Meteor. Res*., 1, 16-24.

Cooley, J.W., and J.W. Tukey, 1965: An algorithm for the machine calculation of complex Fourier series. *Math. Computation*, **19**, 297-301.

Daley, R. C., C. Girard, J. Henderson, and I. Simmonds, 1976: Short-term forecasting with a multi-level spectral primitive equation model. Part I: Model formulation. *Atmosphere*, **14**, 98-116.

DeMaria, M., and R.W. Jones, 1993: Optimation of a hurricane track forecast model with the adjoint model equations. *Mon. Wea. Rev*., **121**, 1730-1745.

Dong, K., and C.J. Neumann, 1986: The relationship between tropical cyclone motion and environmental geostrophic flows. *Mon. Wea. Rev*., **114**, 115-122.

Eliasen, E., B. Machenhauer and E. Ramussen, 1970: On a numerical method for the integration of the hydrodynamical equations with a spectral representation of the horizontal fields. *Rep. No. 2* Institut for Teoretisk Meteorologi, Univ. of Copenhagen.

Ellsaesser, H. W., 1966: Evaluation of spectral versus grid methods of hemispheric numerical weather prediction. *J. Appl. Meteor*., **5**, 246-262.

Evans, J.L., and K. McKinley, 1998: Relative Timing of Tropical Storm Lifetime Maximum Intensity and Track Recurvature. *Meteorol. Atmos. Phys*., **65** 241-245.

Fiorino, M., and R.L. Elsberry, 1989: Some aspects of vortex structure related to tropical cyclone motion. *J. Atmos. Sci*., **46**, 975-990.

Flatau, M., W.H. Schubert, and D.E. Stevens, 1994: The role of baroclinic processes in tropical cyclone motion: The influence of the vertical tilt. *J. Atmos. Sci*., **51**, 2589-2601.

Harshvardhan, Corsetti, T.G., 1984: *Long-wave parameterization for the UCLA/GLAS GCM*. NASA Tech. Memo. 86072, Goddard Space Flight Center, Greenbelt, MD 20771, 52 pp.

Hodanish, S., and W.M. Gray, 1993: An observational Analysis of Tropical Cyclone Recurvature. *Mon. Wea. Rev*., **121**,2665-2689.

Holland, G.J., 1983: Tropical cyclone motion: Environmental interaction plus a beta effect. *J. Atmos. Sci*., **40**, 328-342.

-----, 1984a: On the Climatology and structure of tropical cyclones in the Australian/Southwest Pacific region. I. Data and tropical storms. *Aust. Meteor. Mag*., **32**, 1-16.

-----, 1984b: On the Climatology and structure of tropical cyclones in the Australian/Southwest Pacific region. II. Hurricanes. *Aust. Meteor. Mag*., **32**, 17-32.

Krishnamurti, T.N. and H. S. Bedi, 1988: Cumulus parameterization and rainfall rates III. *Mon Wea Rev*., **116**, 583-599.

-----, J. Xue, H.S. Bedi, K. Ingles, and D. Oosterhof, 1991: Physical initialization for numerical weather prediction over the tropics. *Tellus*, **43**, 53-81.

-----, H.S. Bedi, and K. Ingles, 1993 Physical initialization using SSM/I rain rates. *Tellus*, **45A**, 247-269.

-----, S. Low-Nam, and R. Pasch, 1983: Cumulus parameterization and rainfall rates II. *Mon. Wea. Rev*., **111**, 815-828.

-----, G.D. Rohaly, and H.S. Bedi, 1994: On the improvement of precipitation forecast skill from physical initialization. *Tellus*, **46A**, 598-614.

-----, H.S. Bedi, G.D. Rohaly, and D. Oosterhof, 1996: Partitioning of the Seasonal Simulation of a Monsoon Climate. *Mon. Wea. Rev*., **124**, 1499-1519.

-----, H.S. Bedi, K.S. Yap, D. Oosterhof, and G. Rohaly, 1992: Recurvature Dynamics of a Typhoon. *Meteorol. Atmos. Phys*., **50**, 105-126.

-----, W. Han, and D. Oosterhof, 1998: Sensitivity of hurricane intensity forecasts to physical initialization. *Meteorol. Atmos. Phys*., **65**, 171-181.

Kanamitsu, M., 1975: On numerical prediction over a global tropical belt. Report No. 75-1, Dept. of Meteorology, Florida State University, Tallahassee, Florida 32306, pp. 1-282.

-----, K. Tada, K. Kudo, N. Sato and S. Isa, 1983: Description of the JMA operational spectral model. *J. Met. Soc. Japan*, **61**, 812-828.

Kuo, H.L., 1965: On formation and intensification of tropical cyclones through latent heat release by cumulus convection. *J. Atmos. Sci*., **22**, 40-63.

Kuo, H.L., 1974: Further studies of the parameterization of the influence of cumulus convection on large-scale flow. *J. Atmos. Sci*., **31**, 1232-1240.

Kutzbach, G., 1979: The thermal theory of Cyclones. *Amer. Meteor. Soc*., 255pp.

Lacis, A. A., and J.E. Hansen, 1974: A parameterization of the absorption of solar radiation in the earth's atmosphere. *J. Atmos. Sci*., **31**, 118-133.

Leith, C.E., 1974: Theoretical skill of Monte Carlo forecasts. *Mon. Wea. Rev*., **102**, 409-418.

Louis, F.F., 1979: A parametric model of the vertical eddy fluxes in the atmosphere, *Bound. Layer Meteor*., **17**, 187-202.

MacVean, M.K., 1983: The effects of horizontal diffusion on baroclinic development in a spectral model. *Quart. J. Roy. Meteor. Soc*., **109**, 771-789.

Madala, R.V., and S.A. Piacsek, 1975: Numerical simulation of asymmetric hurricanes on a beta-plane with vertical shear. *Tellus*, **27**, 453-468.

Malkus, J.S., and H. Riehl, 1960: On the dynamics and energy transformations in steady-state hurricanes. *Tellus*, **12**, 1-20.

Orszag, S.A., 1970: Transform method for the calculation of vector-coupled sums: application to the spectral form of the vorticity equation. *J. Atmos. Sci.*, **27**, 890-895.

Platzman, G.W., 1960: The spectral form of the Vorticity equation. *J. Meteorol*., **17**, 635-644.

Phillips, N.A., 1957: A coordinate system having some special advantages for numerical forecasting. *J. Meteor*., **14**, 184-185.

Riehl, H., 1972: Intensity of recurved typhoons. *J. Appl. Meteor*., **11**, 613-615.

-----, and N.M. Burgner, 1950: Further studies on the movement and formation of hurricanes and their forecasting. *Bull. Amer. Meteor. Soc*., **31**, 244-253.

Rossby, C.-G., 1949: On the mechanism for the release of potential energy in the atmosphere. *J. Meteor*., **6**, 163-180.

Sanders, F., and R.W. Burpee, 1968: Experiments in barotropic hurricane track forecasting. *J. Appl. Meteor*., **7**, 313-323.

Shapiro, L.J., 1992: Hurricane Vortex Motion and Evolution in a Three-Layer Model. *J. Atmos. Sci*., **49**, 140-153.

-----, A.C. Pike and J.P. Gaertner, 1975: A barotropic model for operational prediction of tracks of tropical storms. J. Appl. Meteor., 14, 265-280.

Sinnott, R.W., 1984: Virtues of the Haversine. *Sky and Telescope*, **68**, 159.

Slingo J.M., 1987: The development and verification of a cloud prediction scheme for the ECMWF model. *Quart. J. Roy. Meteor. Soc*, **113**, 899-927.

Taylor, G.I., 1916: Skin friction of the wind on the earth's surface. *Proc. Roy. Soc. London*, **A92**, p. 196.

Tiedke, M., 1984: The sensitivity of the time-mean large-scale flow to cumulus convection in the ECMWF model. *Workshop on convection in large-scale numerical models*. ECMWF, 28 Nov.-1 Dec. 1983, 297-316.

Vanderman, L.W., 1962: An improved NWP model for forecasting the paths of tropical cyclones. *Mon. Wea. Rev*., **90**, 19-22.

Vines, B., 1898: Investigation of the cyclonic circulation and translatory movement of West Indian Hurricanes. U.S. Weather Bureau Bulletin No. 11, part 4, 34pp.

Wai, M.M.K., and T.N. Krishnamurti, 1992: An improvement in cumulus parameterization by invoking outgoing longwave radiation. *Meteorol. Atmos. Phys*., **50**, 175-187.

Wallace, J. M., S. Tibaldi, and A.J. Simmons, 1983: Reduction of systematic forecast errors in the ECMWF model through the introduction of envelope orography. *Quart. J. Roy. Meteor. Soc*., **109**, 683-718.

Wang, Y., and G.J. Holland, 1995: Baroclinic dynamics of simulated tropical cyclone recurvature. *J. Atmos. Sci.*, **52**, 410-425.

Williams, R.T., and J.C.-L. Chan, 1994: Numerical studies of the beta effect in tropical cyclone motion. Part II. Zonal mean flow. *J. Atmos. Sci*., **51**, 1065-1076.

Willoughby, H.E., 1998: Tropical cyclone eye thermodynamics. *Mon. Wea. Rev.*, **126**, 3053-3067.

Yanai, M., S. Esbensen, J.H. Chu, 1973: Determination of bulk properties of tropical cloud clusters from large-scale heat and moisture budgets. *J. Atmos. Sci*., **30**, 611-627.

Appendix I. Outline of the FSU Global Spectral Model

(a) Independent variables: (x, y, σ, t)

(b) Dependent variables: Vorticity, divergence, surface pressure, vertical velocity, temperature, and humidity.

(c) Horizontal Resolution: Triangular Truncation at 126 waves.

(d) Vertical resolution: 14 layers between 50 and 1000 hPa.

(e) Semi-implicit time differencing scheme.

(f) Envelope orography (Wallace *et al*., 1983).

(g) Centered differences in the vertical for all variables expect humidity which is handled by an upstream differencing scheme.

(h) Fourth-order horizontal diffusion (Kanamitsu *et al*., 1983).

(i) Kuo-type cumulus parameterization (Kuo, 1965, 1974; Krishnamurti *et al*., 1983)

(j) Shallow convection (Tiedtke, 1984).

(k) Dry convective adjustment.

(l) Large scale condensation (Kanamitsu, 1975).

(m) Surface fluxes via similarity theory (Businger *et al*., 1971).

(n) Vertical distribution of fluxes utilizing diffusive formulation where the exchange coefficients are functions of the Richardson number (Louis, 1979).

(o) Long and short-wave radiative fluxes based on a band model (Harshvardhan and Corsetti, 1984; Lacis and Hansen, 1974).

(p) Diurnal cycle with respect to the radiative processes.

(q) Parameterization of low, middle, and high clouds based on threshold relative humidity for radiative transfer calculations.

(r) Surface energy balance coupled with similarity theory (Krishnamurti *et al*., 1991).

(s) Physical Initialization (Krishnamurti *et al*., 1991).

List of Tables

List of Figures

Figure 10 : Same as figure 4. except for Radiation only. The contour interval is 1.0

Figure 11 : Same as figure 4. except for Shallow Convection and Surface Fluxes only. The contour interval is 2

Figure 12 : Sea level pressure minima-based tracks of all partitions with at least deep convection and total dynamics

Figure 13 : Sea-level pressure minima-based tracks for all partitions without deep convection

Figure 14 : Sea level pressure minima-based tracks of all partitions with at least deep convection and total dynamics

Figure 15 : Sea-level pressure minima-based tracks for all partitions without deep convection

Figure 16 : Sea level pressure minima-based tracks of all partitions with at least deep convection and total dynamics

Figure 17 : Sea-level pressure minima-based tracks for all partitions without deep convection

Figure 18 : Sea level pressure minima-based tracks of all partitions with at least deep convection and total dynamics

Figure 19 : Sea-level pressure minima-based tracks for all partitions without deep convection

Figure 20 : Track errors for both cases of Cindy for the partitions that include deep convection and total dynamics at minimum

Table 1: Model Physics budget – units are hPa per 120 hours

CASE	TOTAL PHYSICS	SUMMED PHYSICS
Cindy – 26 August, 1999	-2.538	-2.464
Dennis – 28 August, 1999	-3.931	-3.759

Table 2. List of Acronyms

AD	(Nonlinear) Advective Dynamics
AFWA	U.S. Air Force Weather Agency
AMS	American Meteorological Society
BAMD	Beta and Advection Model - Deep Depth
BAMM	Beta and Advection Model - Medium Depth
BAMS	Beta and Advection Model - Shallow Depth
CISK	Convective Instability of the Second Kind
CNV	Deep convection partition
DC	TDYN+CNV
DL	DC+LSP
DLR	DL+RAD
DLRS	DLR+SC
DLS	DL+SC
DR	DC+RAD
DRS	DR+SC
DS	DC+SC
ECMWF	European Center for Medium-Range Weather Prediction
FFT	Fast Fourier Transform
FSU	Florida State University
FSUGSM	Florida State University Global Spectral Model
FULL	Full model run (all inclusive)
GCM	General Circulation Model
GLAS	Goddard Laboratory for Atmospheric Studies
hPa	Hecto-Pascal
L/LSP	Large scale precipitation
LR	TDYN+L
LRS	LR+SC

LS	TDYN+LSP+SC
NCEP	National Center for Environmental Predicition
NHC	National Hurricane Center
NOAA	National Oceanic and Atmospheric Administration
NWP	Numerical Weather Prediction
OLR	Outgoing Long wave Radiation
PHY	Physics Partition - all components
PI	Physical Initialization
R/RAD	Radiation partition
RD/RDYN	Rest of the Dynamics – linear component of model dynamics
RS	TDYN+RAD+SC
SAB	Satellite Analysis Branch
S/SC	Shallow Convection (surface fluxes included here) partition
SST	Sea Surface Temperature
TAFB	Tropical Analysis and Forecast Branch
TC	Tropical Cyclone
TD	Tropical Depression
TDYN	Total Dynamics
TPC	Tropical Prediction Center
TPHY	Total Physics
TS	Tropical Storm
UCLA	University of California at Los Angeles
VICBAR	Barotropic track model utilizing shallow water equations

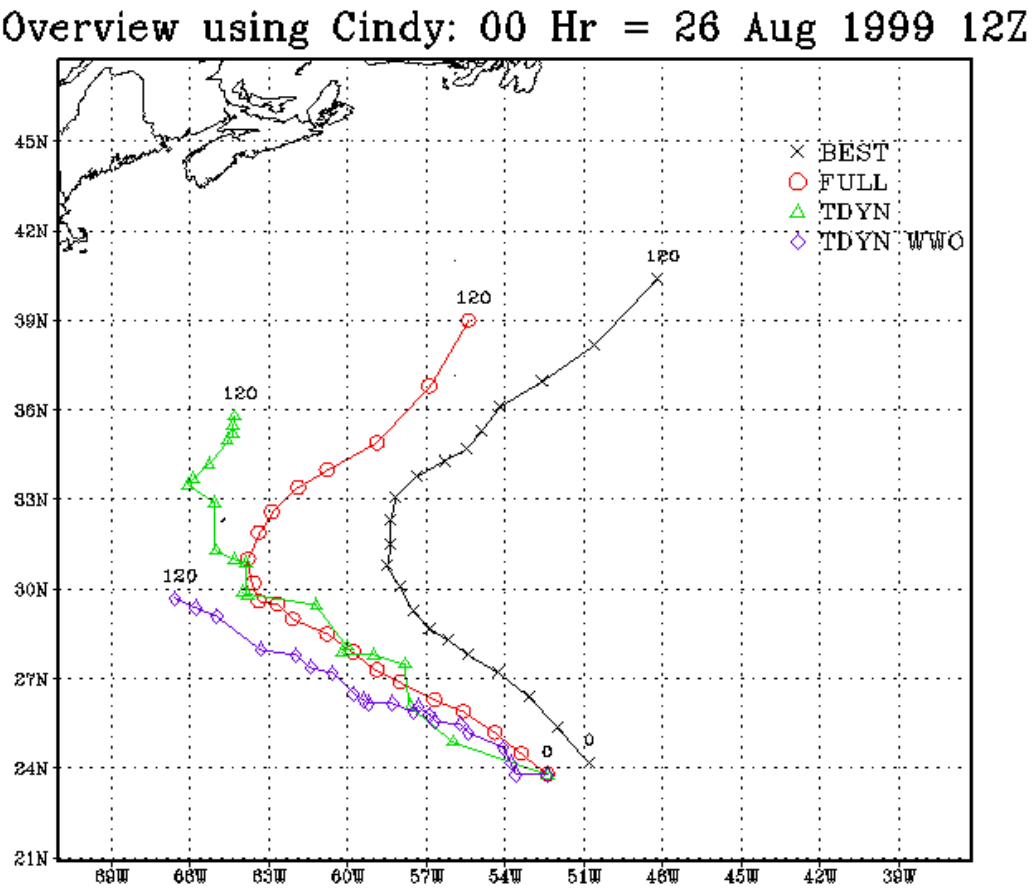

Figure 1. Illustration of the track difference between the full dynamics of the 'with and with' notion (TDYN) and the full dynamics using a 'with and without' technique (TDYN WWO)

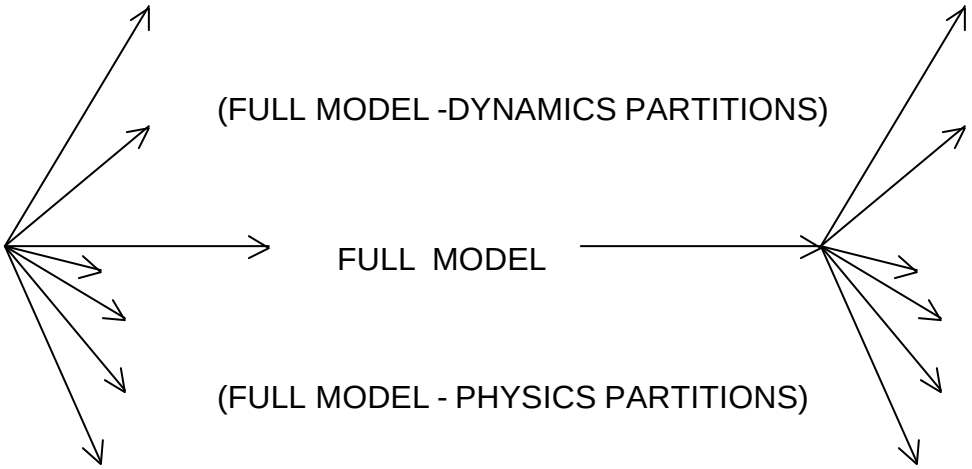

Figure 2. Illustration of the partition configuration with the full model as input for each integrated time-step

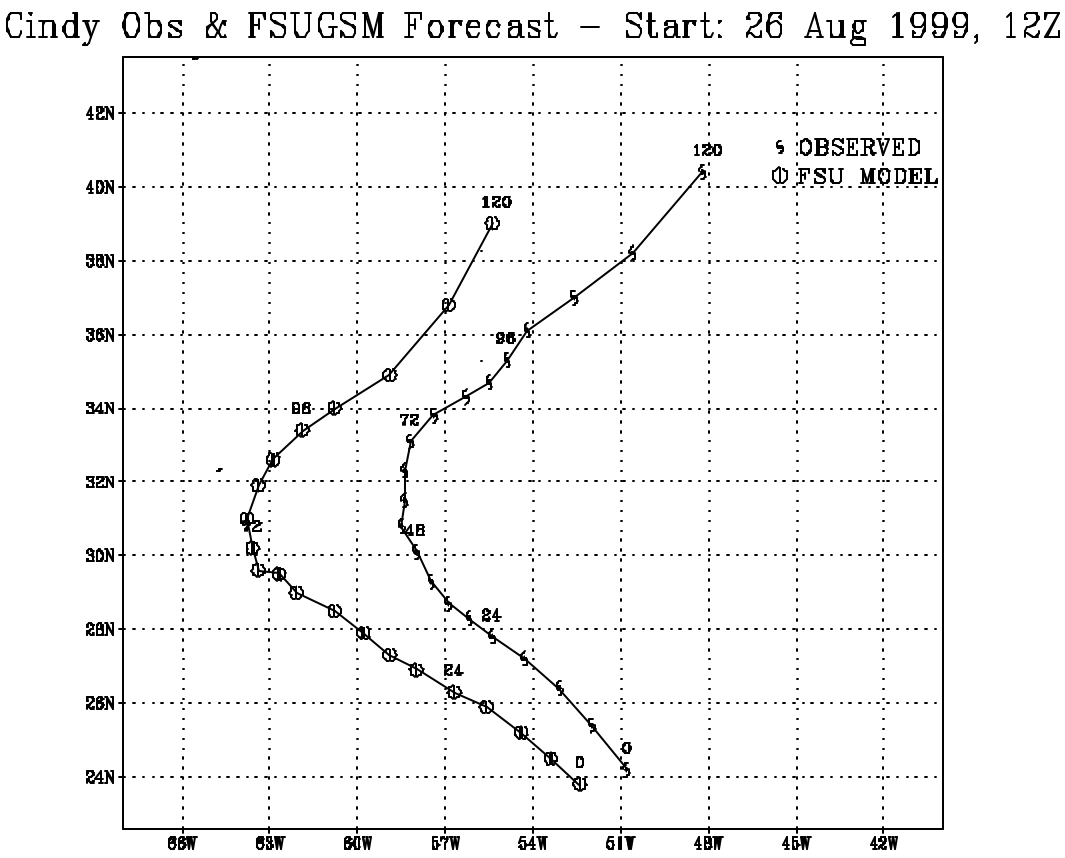

Figure 3: Hurricane Cindy best track and FSU-GSM forecasts beginning 26 August 1999, at 12Z.

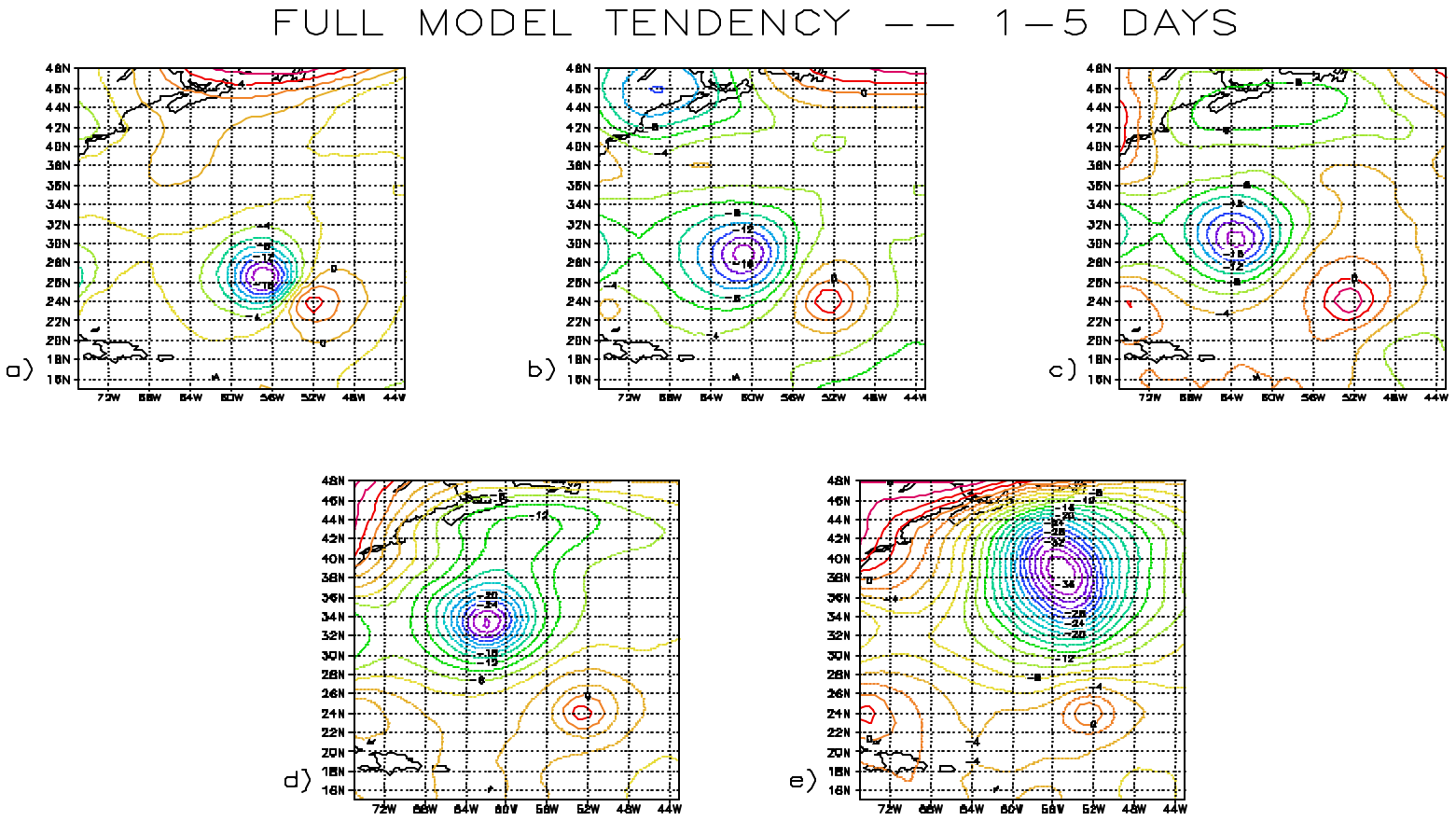

Figure 4: Hurricane Cindy (Julian Day = 238) full model, Sea Level Pressure tendency contribution in 24 hour increments, with a) 24 hour tendency, b) 48 hour tendency, c) 72 hour tendency, d) 96 hour tendency and e) 120 hour tendency. All contours are in units of hPa per respective time period - the contour interval is 2 hPa.

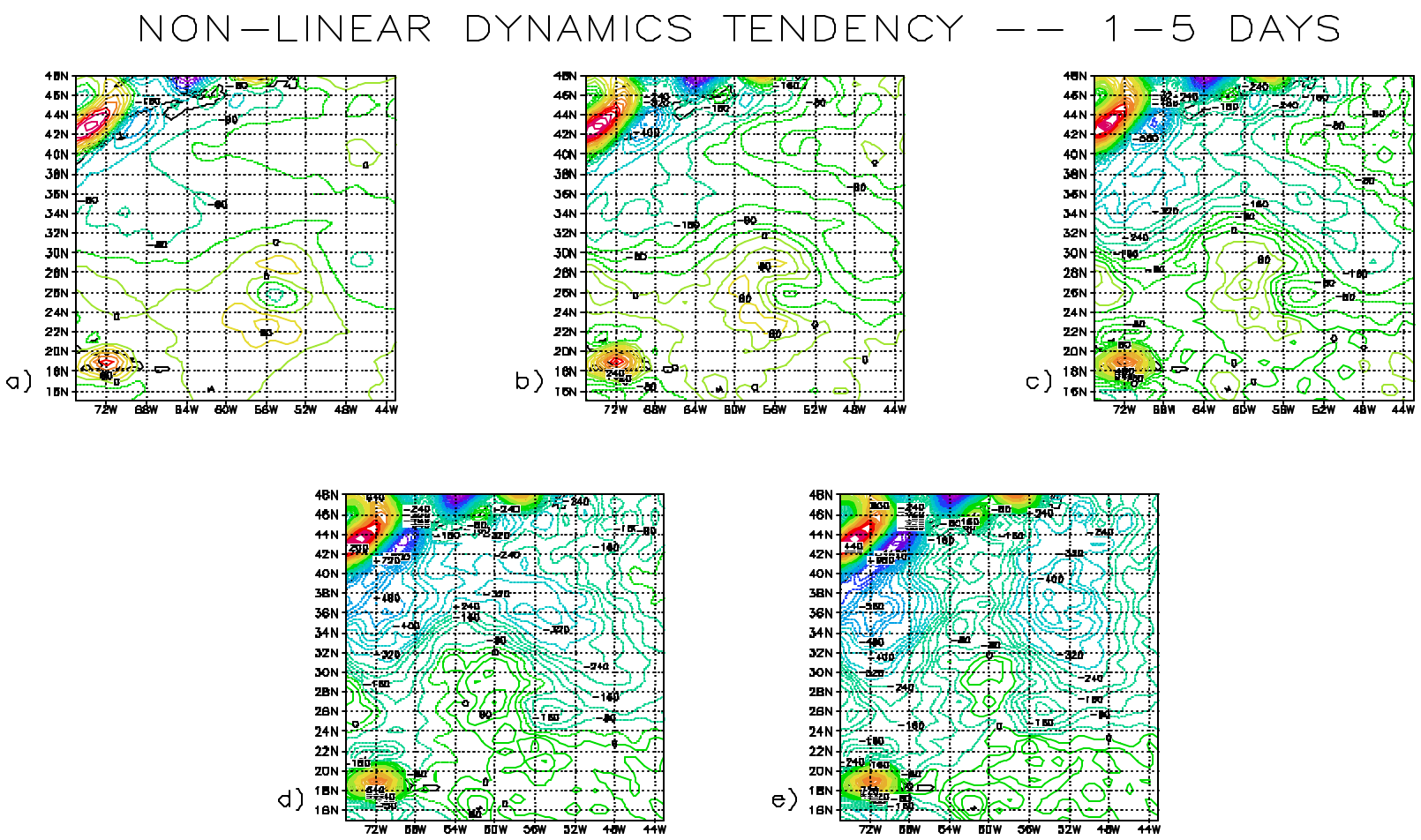

Figure 5: Same as figure 4. except for Non-Linear Advective Dynamics only. The contour interval is 40.

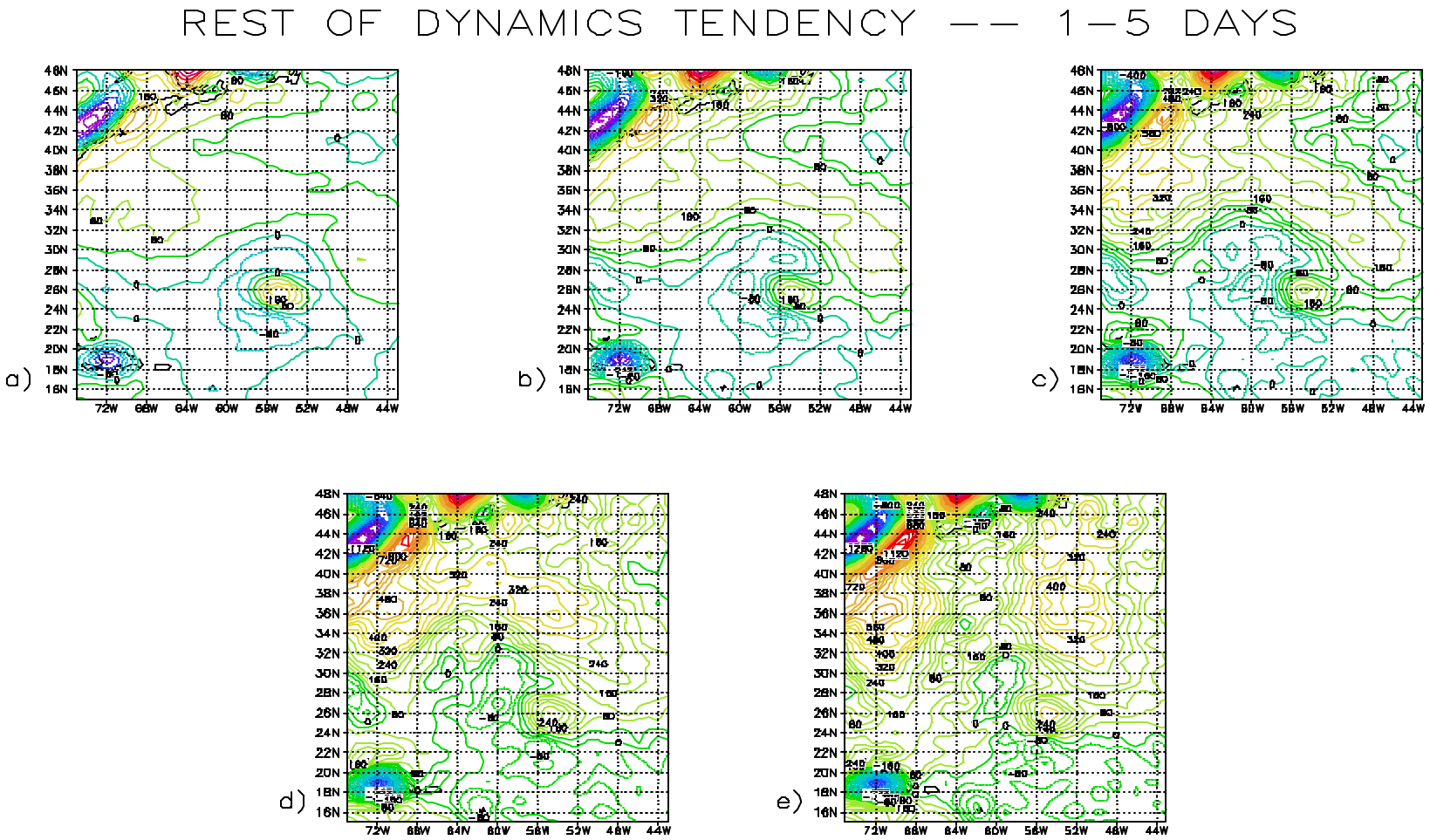

Figure 6: Same as figure 4. except for Linear Dynamics (rest of dynamics) only. The contour interval is 40.

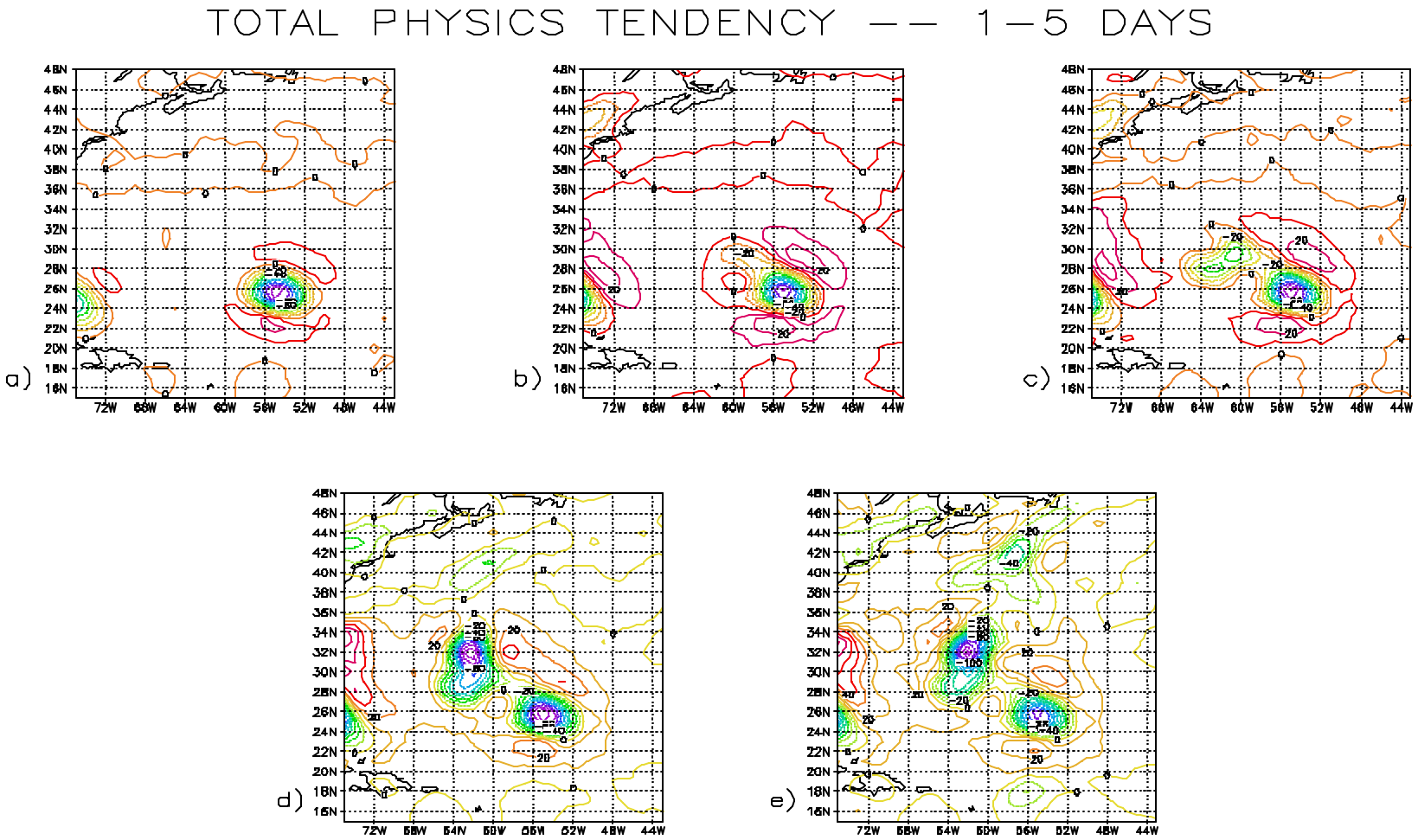

Figure 7: Same as figure 4. except for Total Physics only. The contour interval is 10.

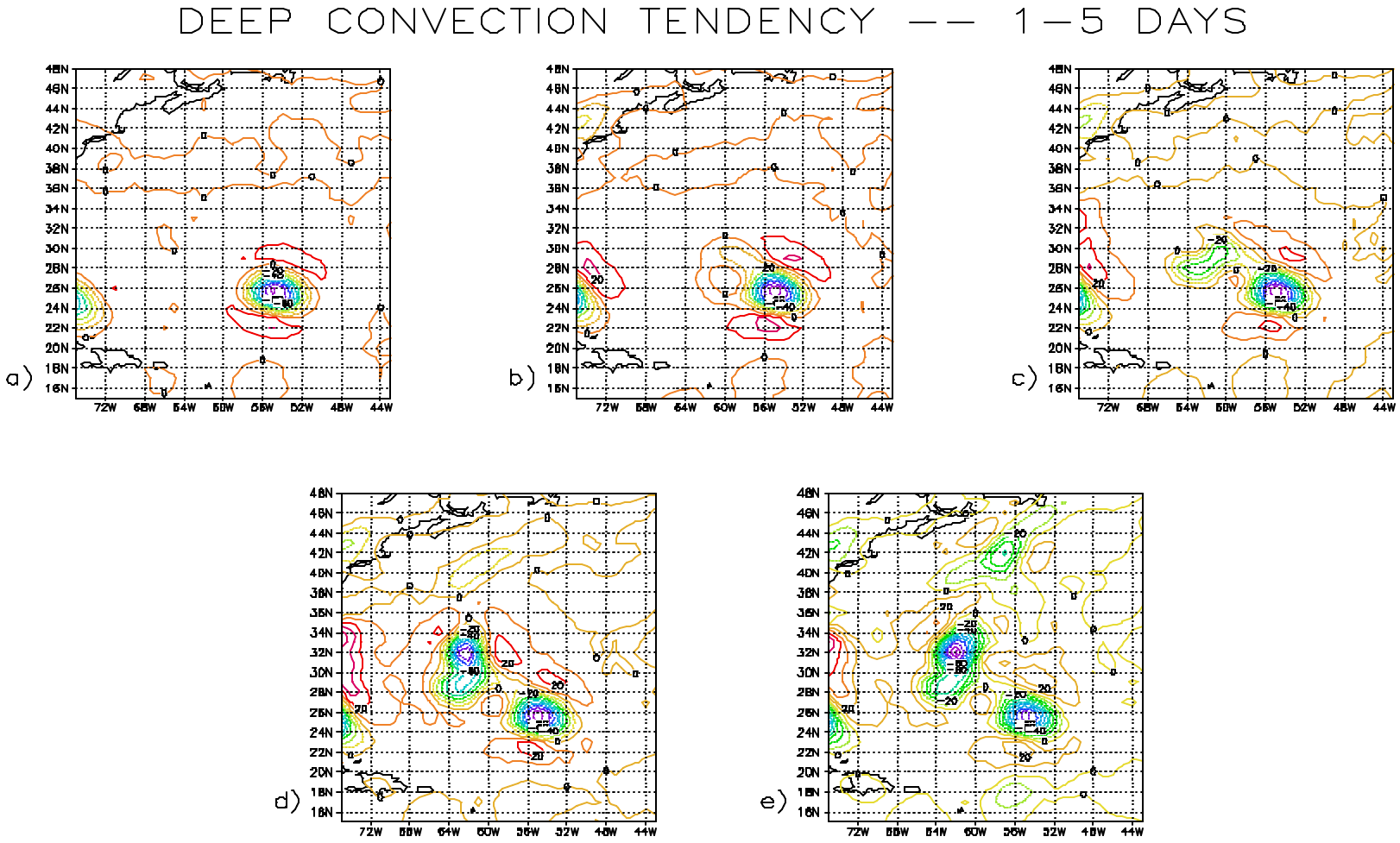

Figure 8: Same as figure 4. except for Deep Convection only. The contour interval is 10.

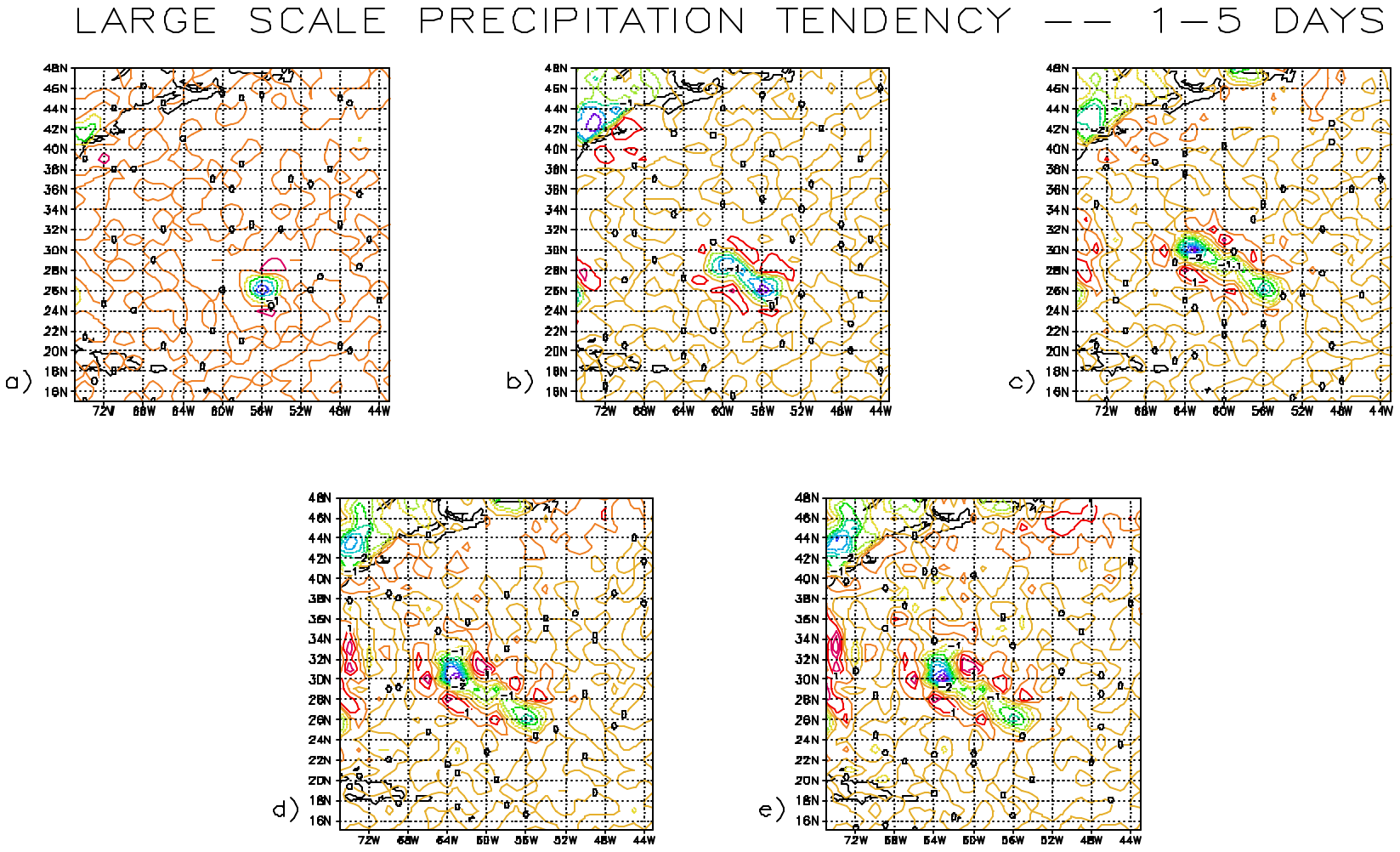

Figure 9: Same as figure 4. except for Large Scale Precipitation only. The contour interval is 1.0.

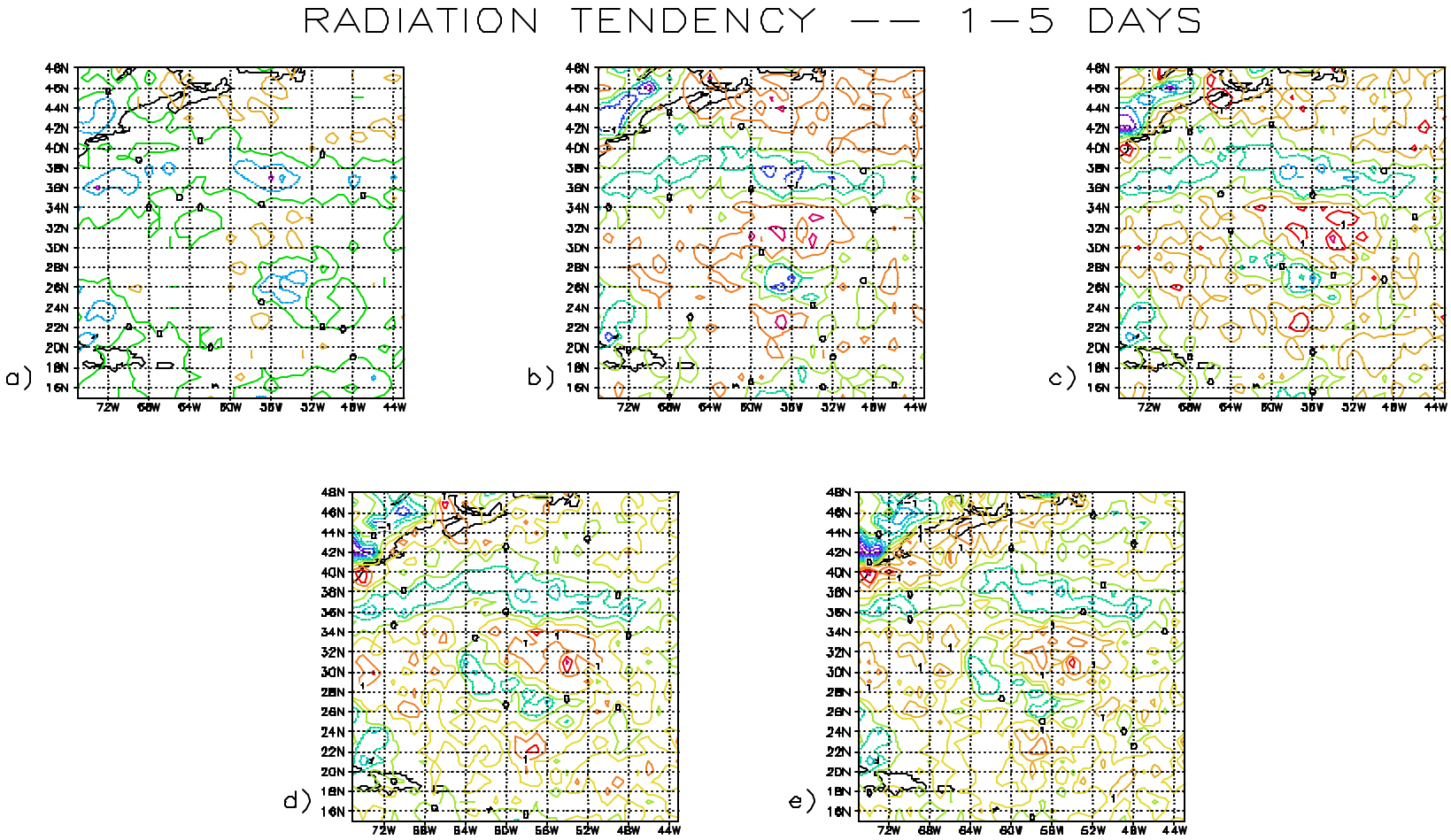

Figure 10: Same as figure 4. except for Radiation only. The contour interval is 1.0.

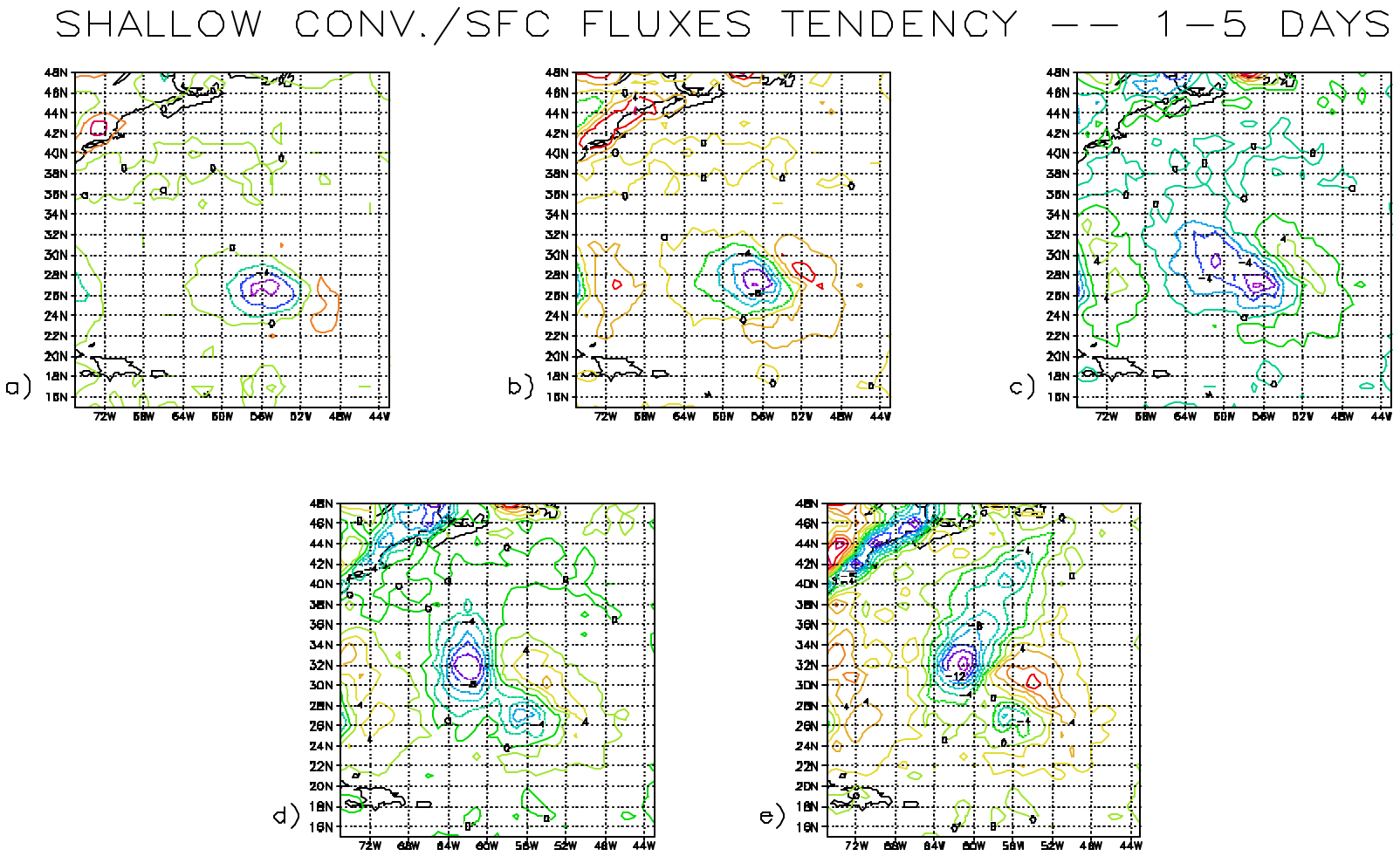

Figure 11: Same as figure 4. except for Shallow Convection and Surface Fluxes only. The contour interval is 2.

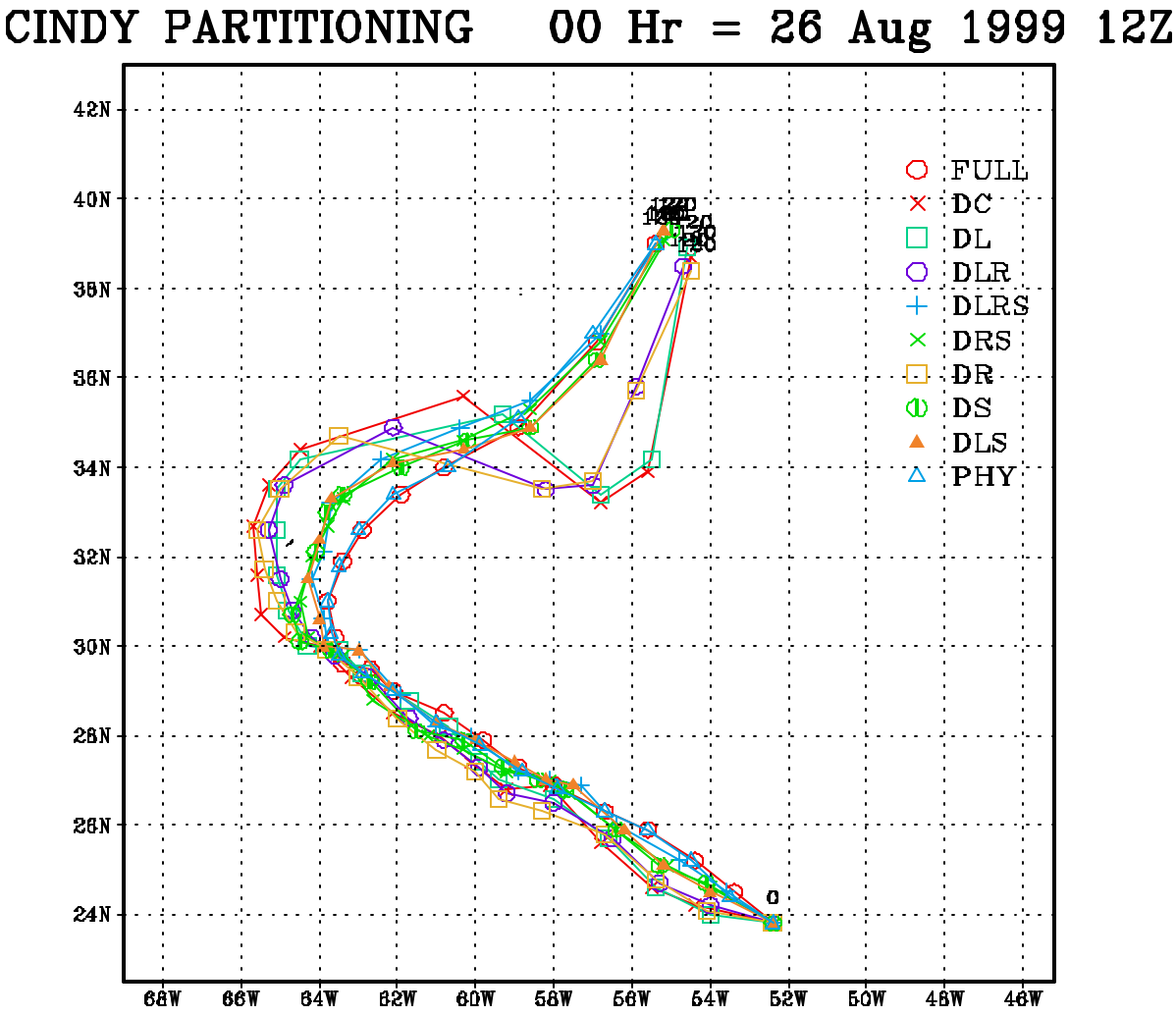

Figure 12: Sea level pressure minima-based tracks of all partitions with at least deep convection and total dynamics.

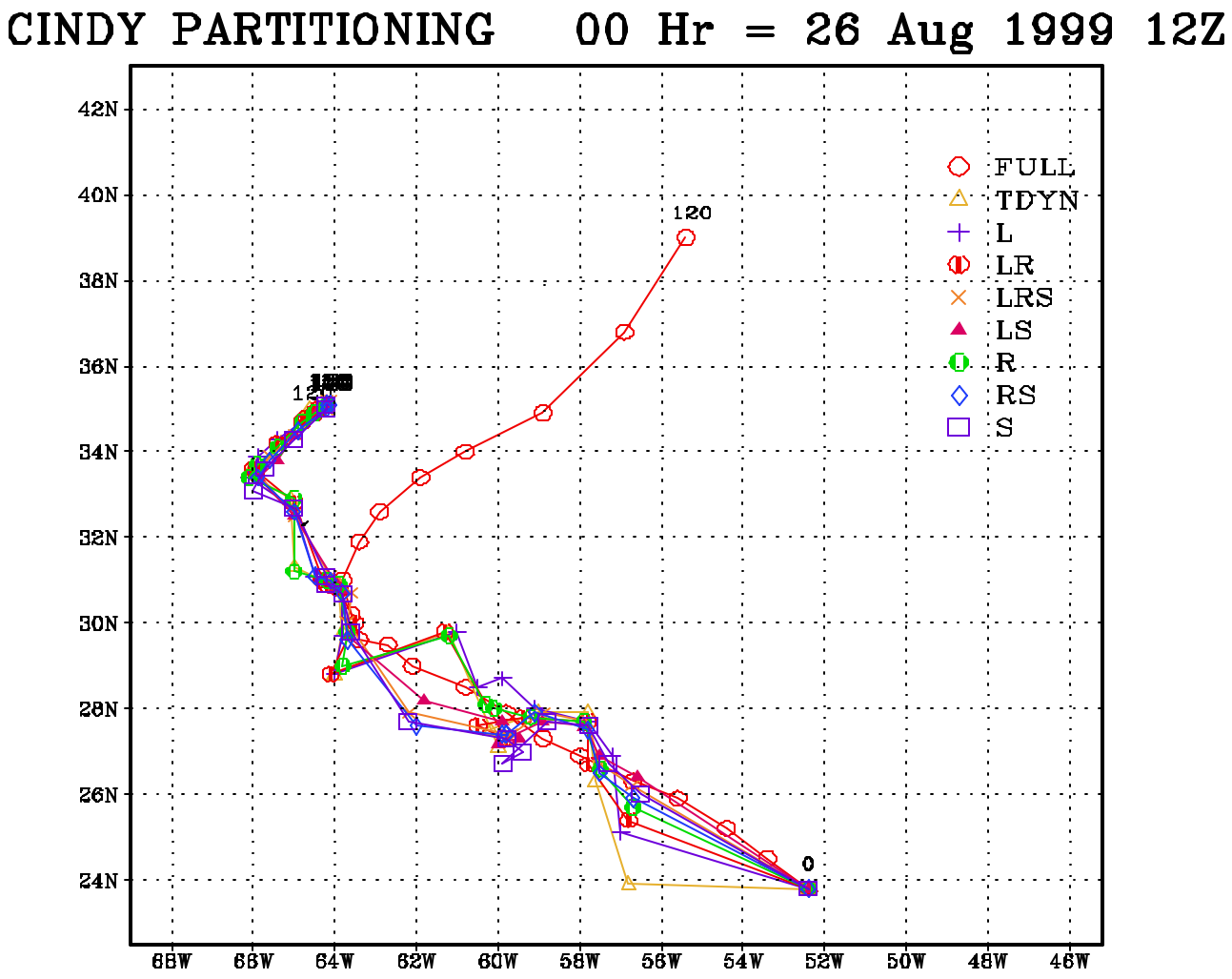

Figure 13: Sea-level pressure minima-based tracks for all partitions without deep convection.

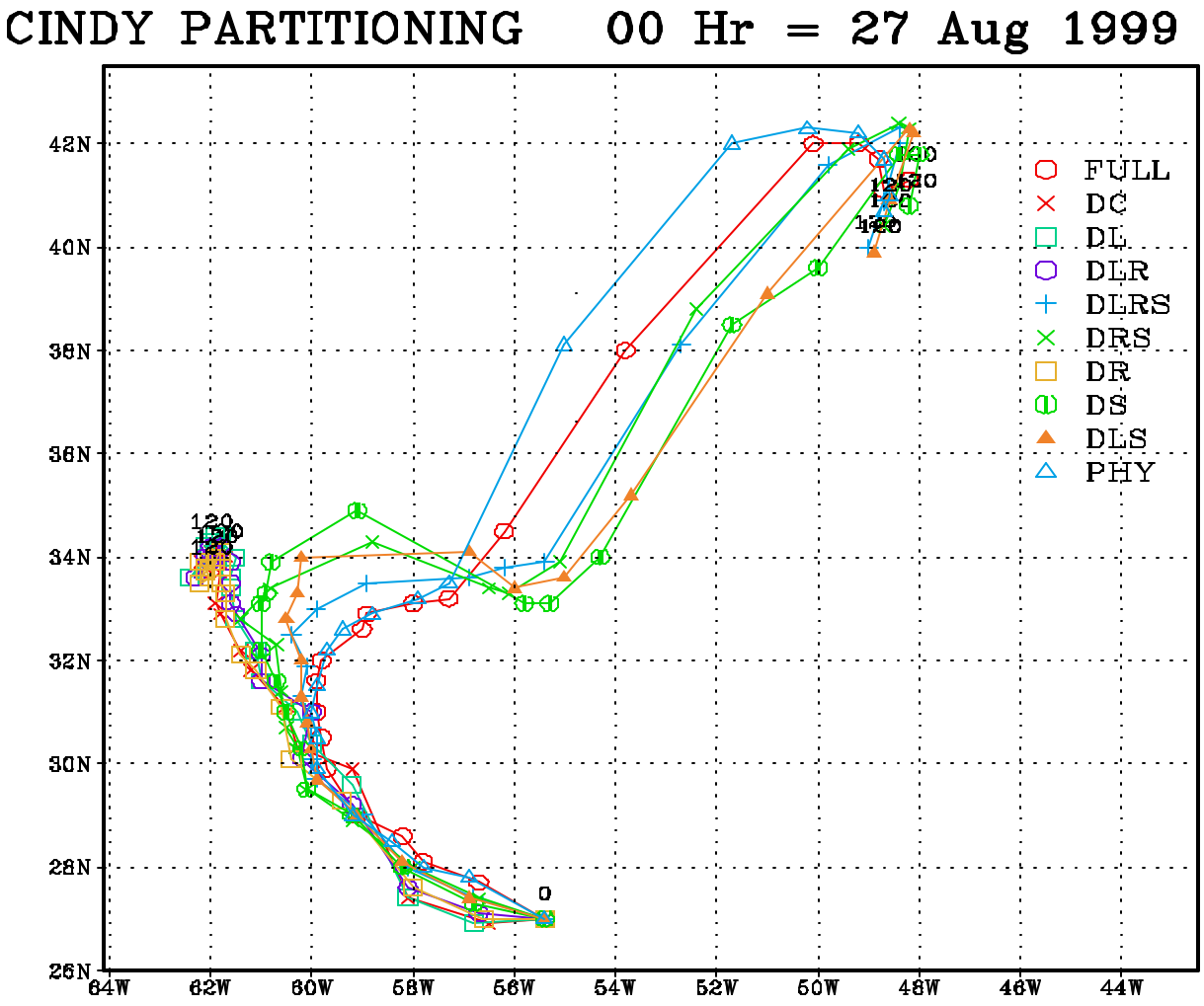

Figure 14: Sea level pressure minima-based tracks of all partitions with at least deep convection and total dynamics.

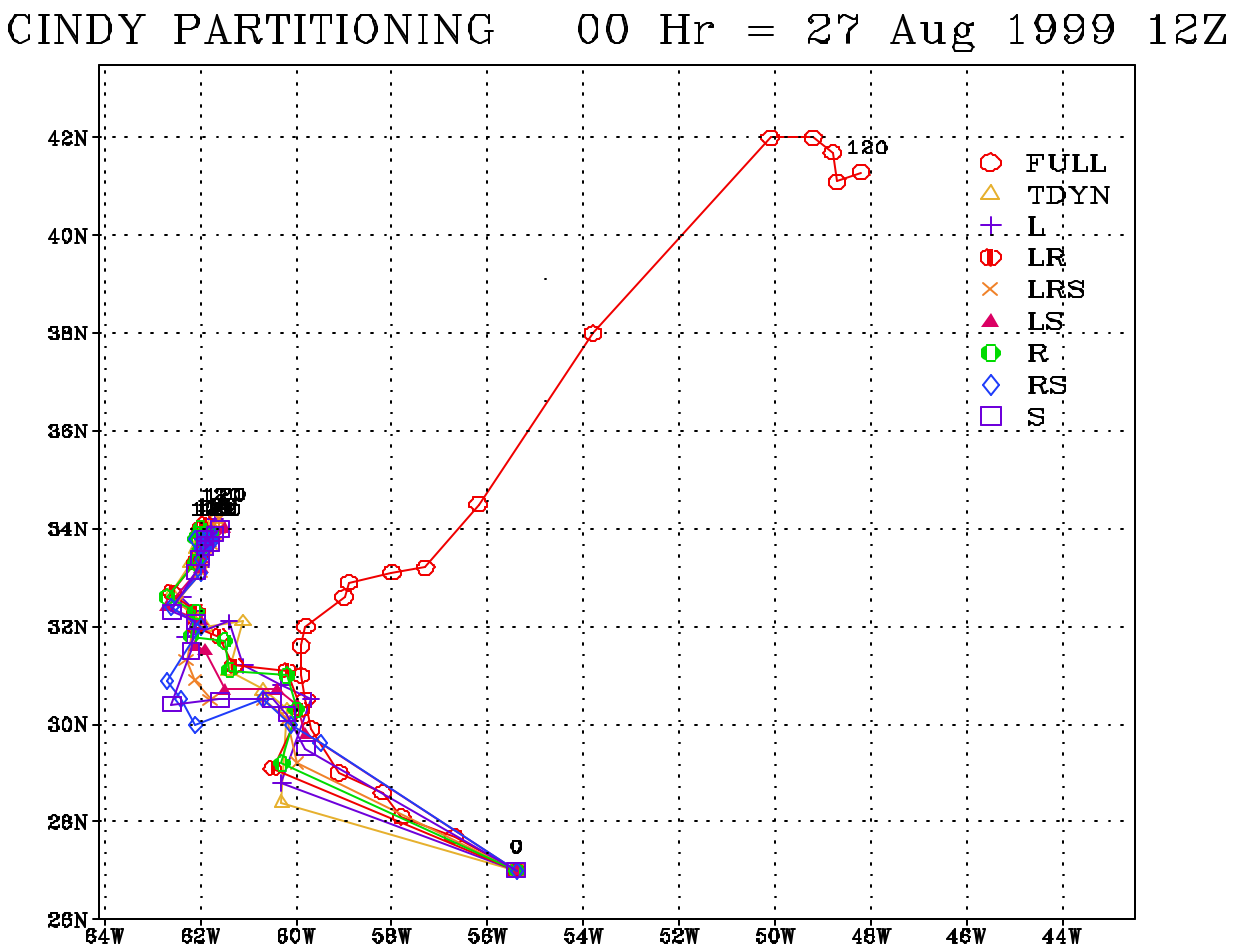

Figure 15: Sea-level pressure minima-based tracks for all partitions without deep convection.

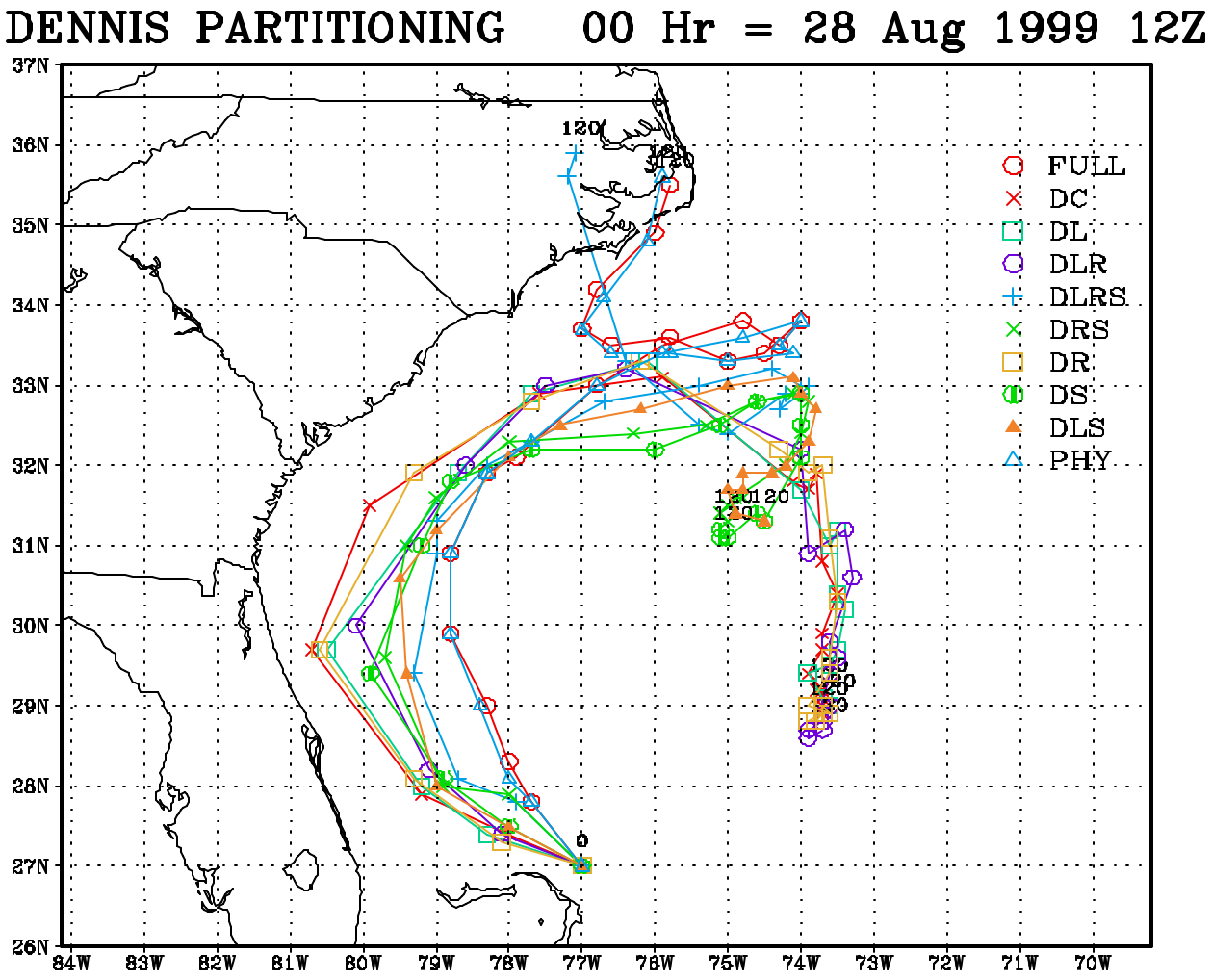

Figure 16: Sea level pressure minima-based tracks of all partitions with at least deep convection and total dynamics.

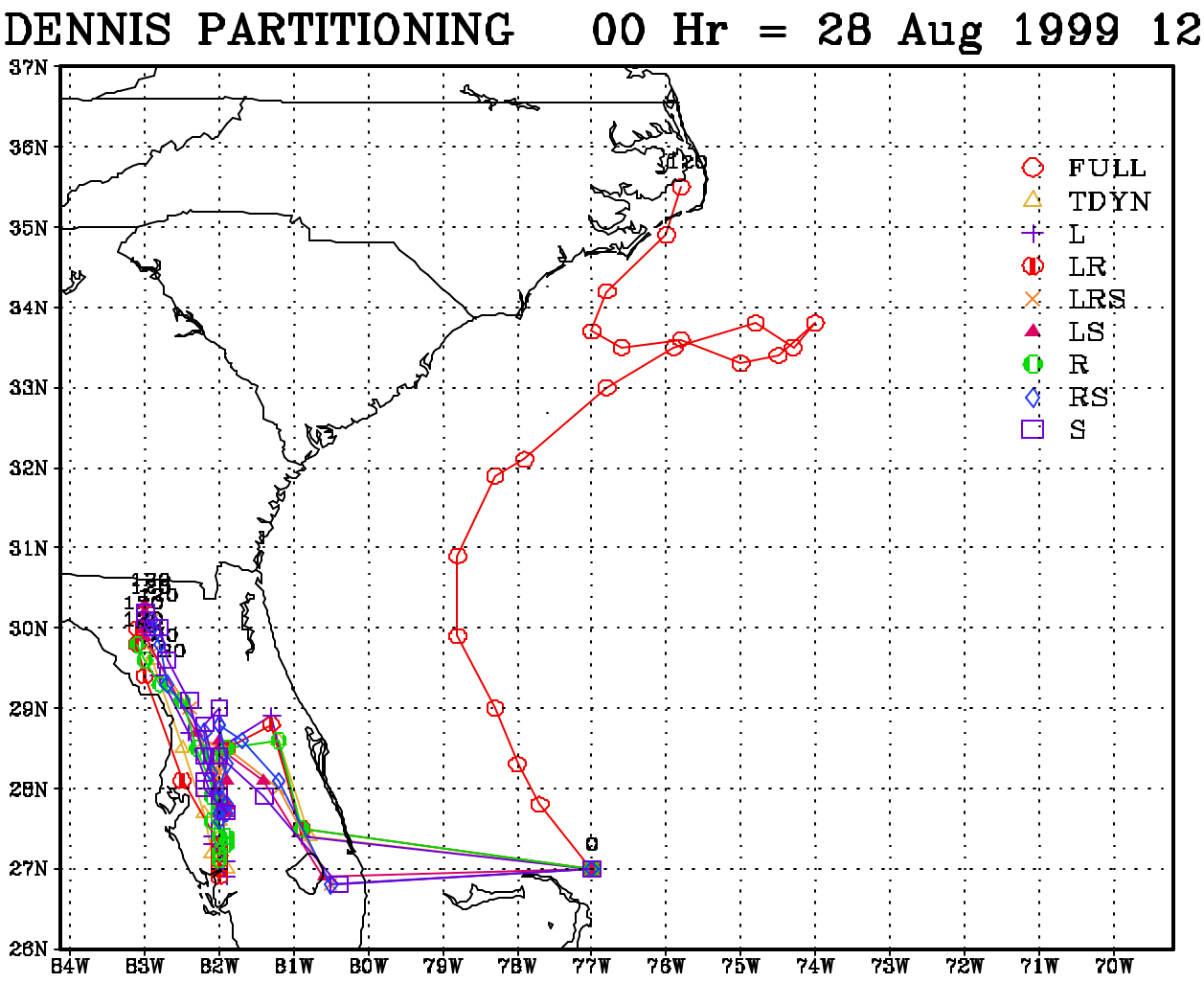

Figure 17: Sea-level pressure minima-based tracks for all partitions without deep convection.

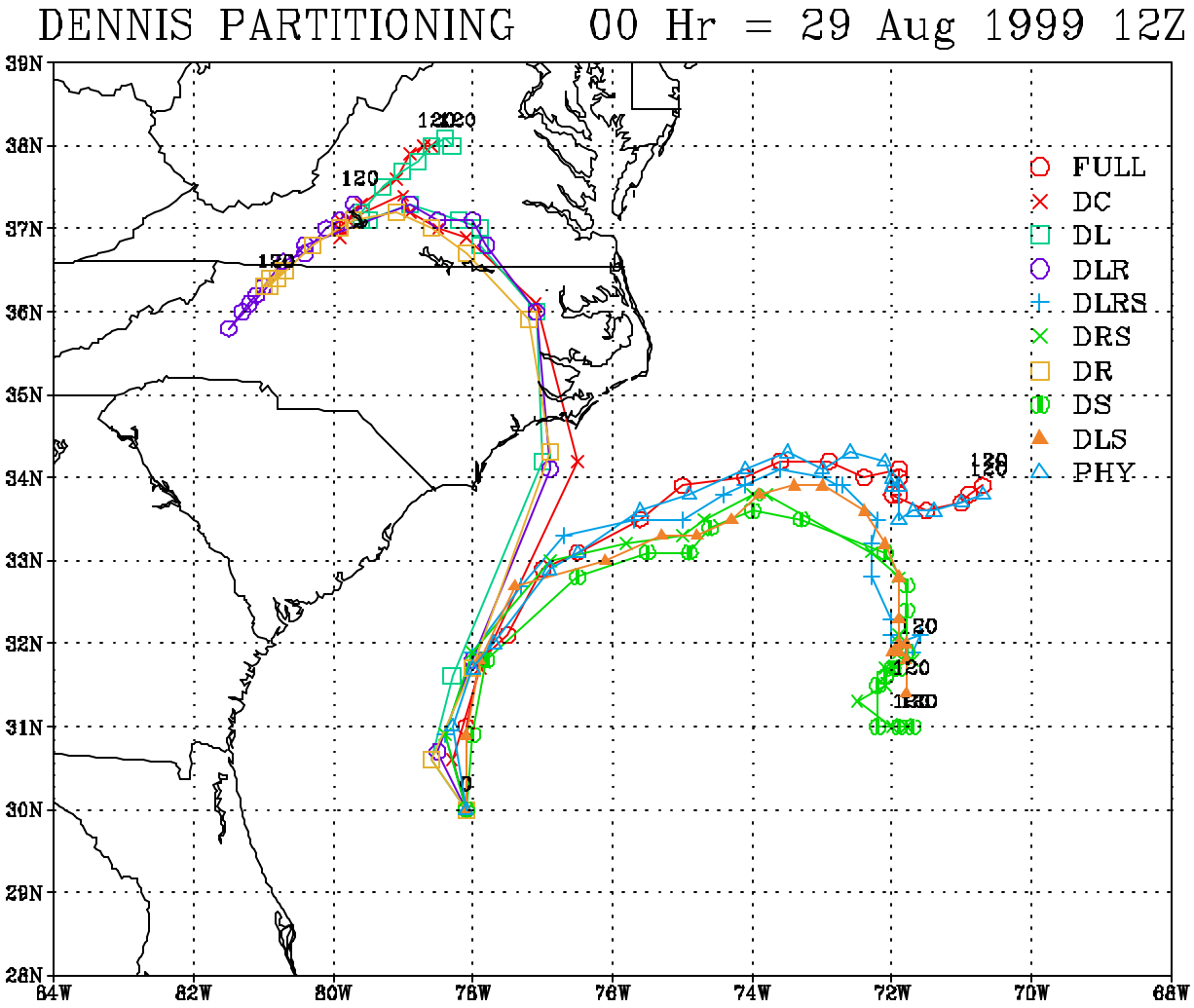

Figure 18: Sea level pressure minima-based tracks of all partitions with at least deep convection and total dynamics.

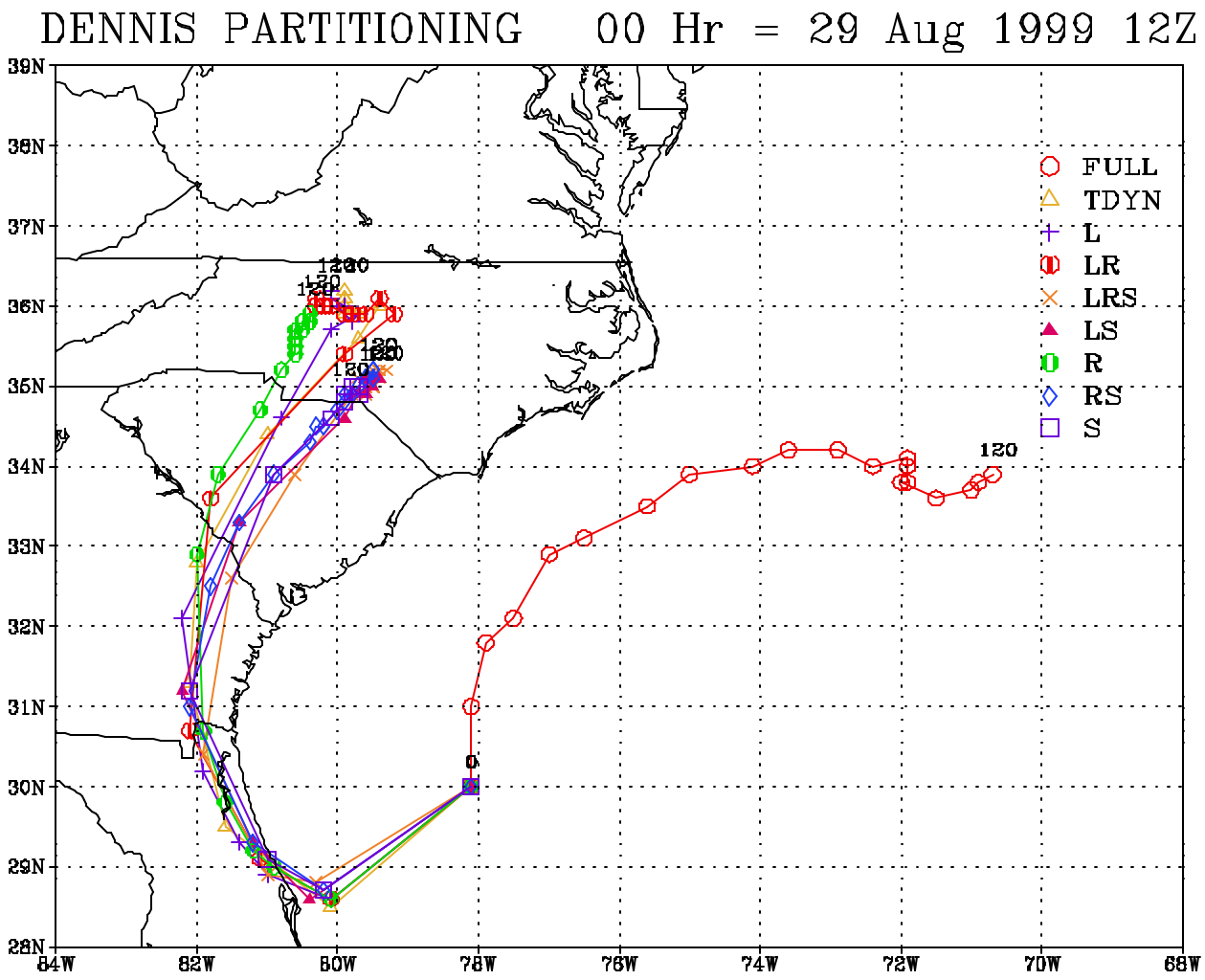

Figure 19: Sea-level pressure minima-based tracks for all partitions without deep convection.

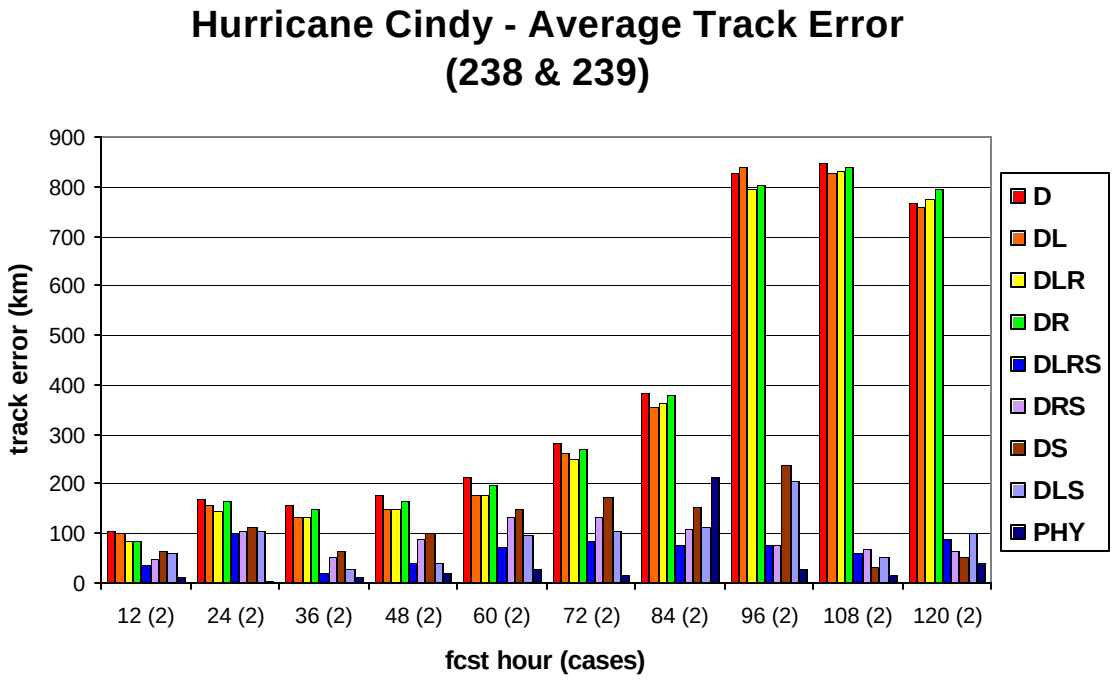

Figure 20: Track errors for both cases of Cindy for the partitions that include deep convection and total dynamics at minimum.

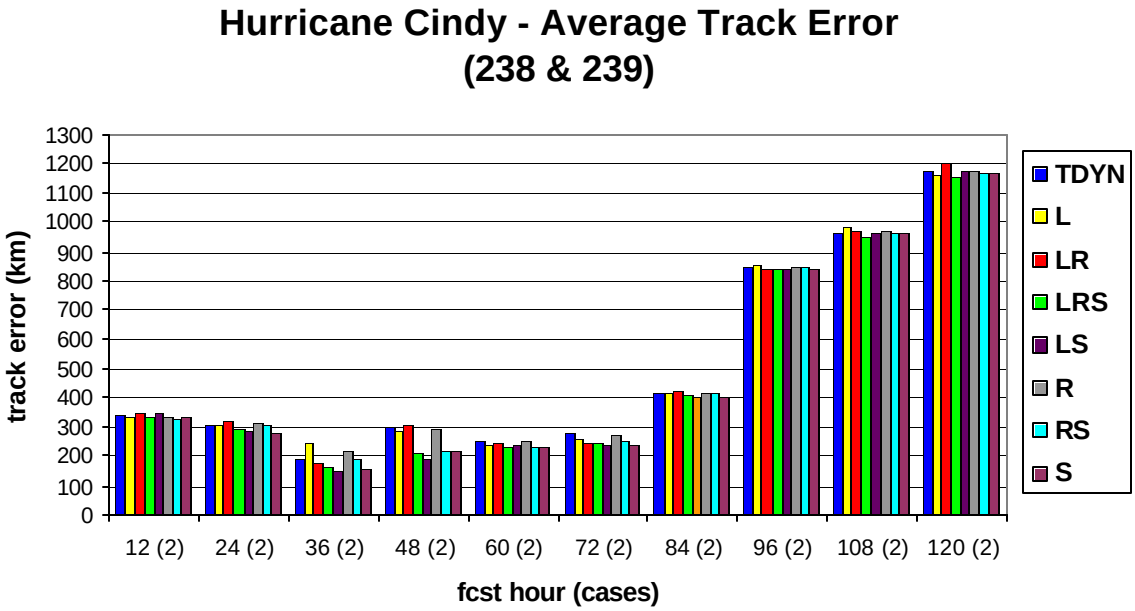

Figure 21: Track errors for both cases of Cindy for the partitions that include total dynamics at minimum – without deep convection.

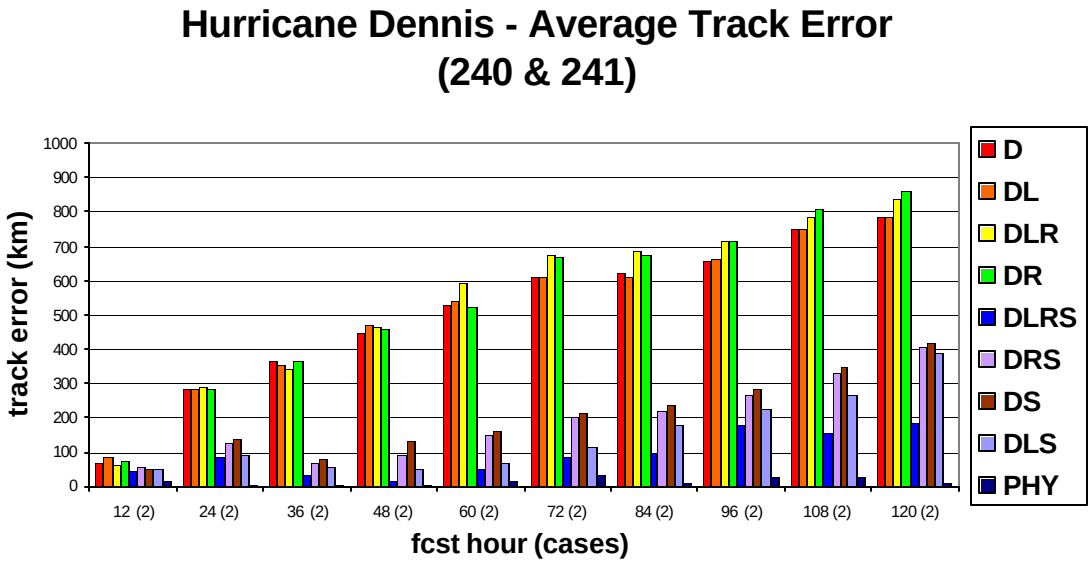

Figure 22: Track errors for both cases of Dennis for the partitions that include deep convection and total dynamics at minimum.

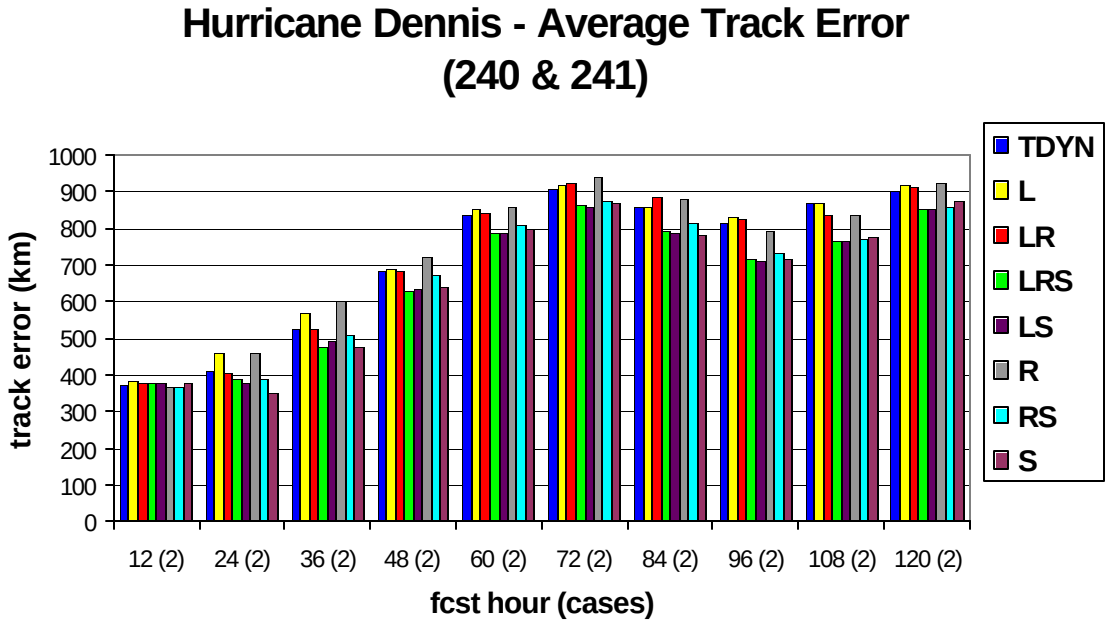

Figure 23: Track errors for both cases of Dennis for the partitions that include total dynamics at minimum – without deep convection.